Comparative study between a two-group and a multi-group energy dynamics code

Louisa Pretorius

Mini-dissertation submitted in partial fulfilment of the requirements for the degree Master of Engineering at the Potchefstroom Campus of the North-West University

Supervisor: Prof. Eben Mulder

November 2010

Innovation through diversity

NORTH-WEST UNIVERSITY
YUNIBESITI YA BOKONE-BOPHIRIMA
NOORDWES-UNIVERSITEIT
POTCHEFSTROOM CAMPUS

ABSTRACT

Name: Louisa Pretorius

Title: Comparative study between a two-group and a multi-group energy dynamics code

Date: November 2010

The purpose of this study is to evaluate the effects and importance of different cross-section representations and energy group structures for steady state and transient analysis. More energy groups may be more accurate, but the calculation becomes much more expensive, hence a balance between accuracy and calculation effort must be find.

This study is aimed at comparing a multi-group energy dynamics code, MGT (Multi-group TINTE) with TINTE (TIme Dependent Neutronics and TEmperatures). TINTE's original version (version 204d) only distinguishes between two energy group structures, namely thermal and fast region with a polynomial reconstruction of cross-sections pre-calculated as a function of different conditions and temperatures. MGT is a TINTE derivative that has been developed, allowing a variable number of broad energy groups.

The MGT code will be benchmarked against the OECD PBMR coupled neutronics/thermal hydraulics transient benchmark: the PBMR-400 core design. This comparative study reveals the variations in the results when using two different methods for cross-section generation and multi-group energy structure. Inputs and results received from PBMR (Pty) Ltd. were used to do the comparison.

A comparison was done between two-group TINTE and the equivalent two energy groups in MGT as well as between 4, 6 and 8 energy groups in MGT with the different cross-section generation methods, namely inline spectrum- and tabulated cross-section method. The characteristics that are compared are reactor power, moderation- and maximum fuel temperatures and k-effective (only steady state case).

This study revealed that a balance between accuracy and calculation effort can be met by using a 4-group energy group structure. A larger part of the available increase in accuracy can be obtained with 4-groups, at the cost of only a small increase in CPU time.

The changing of the group structures in the steady state case from 2 to 8 groups has a greater influence on the variation in the results than the cross-section generation method that was

used to obtain the results. In the case of a transient calculation, the cross-section generation method has a greater influence on the variation in the results than on the steady state case and has a similar effect to the number of energy groups.

Keywords: TINTE, Multi-group TINTE, energy group structure, steady state, transient.

UITTREKSEL

Naam: Louisa Pretorius

Titel: Vergelykende studie tussen ‘n 2-groep en ‘n multi-group energie dinamiese kode

Datum: November 2010

Die doel van hierdie studie is om die effek en belangrikheid van verskillende dwarsdeursnit-area voorstellings en energiegroep-strukture vir tyd onafhanklike en transiente analises te evalueer. Meer energiegroepe mag meer akkuraat wees, maar die berekening daarvan word veel duurder, derhalwe moet ‘n balans tussen akkuraatheid en berekeningsinspanning gevind word.

Hierdie studie handel oor 'n vergelyking tussen ‘n multi-groep energie dinamiese kode, MGT (Multi-Groep TINTE) en TINTE *(TIme Dependant Neutronics and Temperature)*. TINTE se oorspronklike weergawe het slegs onderskei tussen 'n twee-groep energie indelingstruktuur, naamlik die termiese- en vinnige gebied met 'n twee-groep polinomiese rekonstruksie van deursnit-areas as ‘n funksie van verskillende kondisies en temperature. MGT is afgelei vanaf TINTE om 'n veranderlike aantal energiegroepe te akkommodeer.

Die MGT kode sal gevalideer word teen die *"OECD PBMR coupled neutronics/thermal hydraulics benchmark: PBMR-400 core design".* Hierdie vergelykende studie toon die verskille in die resultate aan wanneer daar van twee verskillende dwarsdeursneë bepaling-metodes, asook multi-groep energie strukture gebruik gemaak word. Insette en resultate verkry vanaf PBMR (Edms) Bpk. is vergelyk.

'n Vergelyking tussen twee-groep TINTE en die ooreenstemmende twee energie groepe in MGT is getref om k-effektief te vergelyk. Daar is ook ‘n vergelyking getref tussen 2, 4, 6 en 8 groepe in MGT, naamlik die deursnit-area bepaling-metodes wat gebruik is in die inlyn spektrum en die getabuleerde deursnit-area metodes. Reaktor krag, moderator- en maksimum brandstoftemperature en k-effektief (slegs in die tyd onafhanklike geval) is vergelyk.

Hierdie studie het getoon dat ‘n balans tussen akkuraatheid en berekeningsinspanning gevind kan word met die gebruik van 4-groep energiegroep-struktuur. ‘n Beter akkuraatheid kan verkry word met 4-groepe, teen slegs ‘n klein verhoging in SVE (Sentrale

Verwerkingseenheid) tyd. Die invloed in verandering van die energiegroep-strukture vanaf 2 na 8 groepe in die tyd onafhanklike geval, het ‘n groter invloed in die variasie in die resultate as die dwarsdeursnit-area voorstellings wat gebruik is om die resultate te verkry. In die transiënte geval het die dwarsdeursnit-area ‘n groter inlvoed op die resultate as in die gestadigde geval, waar die energie-groep indeling ‘n soortgelyke effek het.

Sleutelwoorde: TINTE, Multi-groep TINTE, energie-groep indeling, tyd onafhanklik, transient.

ACKNOWLEDGEMENTS

My heavenly Father, for the talent He gave me to make this study possible, His guidance, strength and inspiration and His helping hand.

Professor Eben Mulder for his assistance and advice through this study.

Everyone at PBMR (Pty) Ltd. for their advice and inputs.

Christel Eastes for the editing of this thesis.

My father, mother, sisters and in-laws, for all their support, interest and encouragement and always being willing to listen.

My dearest husband, Ernst, who knew exactly what I was going through, and was always there for help, advice, encouragement, support and his love to help me complete this study.

TABLE OF CONTENT

LIST OF FIGURES

LIST OF TABLES

ABBREVIATIONS

2D	Two-dimensional
3D	Three-dimensional
AVR	German: Arbeitsgemeinschaft Versuchsreaktor
BR	Bottom Reflector
BWR	Boiling Water Reactor
B4C	Boron Carbide
CANDU	CANada Deuterium Uranium
CB	Core Barrel
CBCS	Core Barrel Conditioning System
CC	Central Column
CR	Control Rod
CRE	Control Rod Ejection
CRP	Coordinated Research Program
CRW	Control Rod Withdrawal
DIN	Deutsches Institut für Normung e. V. (German Institute of Standards)
DLOFC	Depressurized Loss of Forced Cooling
D2O	Deuterium Oxide
eV	Electron Volts
FJZ	Forschungszentrum Jülich
HTGR	High-temperature Gas-cooled Reactor
k-eff	Effective multiplication factor
LWR	Light Water Reactor
MEDUL	MehrfachDUrchLauf (German for recirculation)
MGT	Multi-Group TINTE
NEA	Nuclear Energy Agency
NPP	Nuclear Power Plant
OECD	Organization for Economic Co-operation and Development
PBMR	Pebble Bed Modular Reactor
PBMR (Pty) Ltd.	Pebble Bed Modular Reactor Company (Pty) Ltd.
PLOFC	Pressurized Loss of Forced Cooling

PWR	Pressurized Water Reactor
RCCS	Reactor Cavity Cooling System
RCS	Reactivity Control System
RPV	Reactor Pressure Vessel
RSS	Reserve Shutdown System
SR	Side Reflector
SVE	Sentrale Verwerkingseenheid (Afrikaans for Central Processing Unit)
TCRE	Total Control Rod Ejection
TCRW	Total Control Rod Withdrawal
THTR	Thorium High Temperature Reactor
TINTE	Time Dependent Neutronics and Temperatures
TR	Top Reflector
TRISO	Triple Coated Isotropic Particle
UO_2	Uranium Oxide
VHTR	Very High Temperature Reactor
VSOP	Very Superior Old Program
V&V	Verification and Validation
X-S	Cross-section

1. CHAPTER ONE: INTRODUCTION

Your expectation must not be based on what you are today, but on what you hope to become someday. ***John Maxwell***

1.1 Introduction

The escalating demand for electricity and the depletion of fossil fuel reserves, like coal, natural gas and oil, put the entire world in need of an emission-free, environmentally friendly energy source and -infrastructure to satisfy the world's insatiable hunger for power. Electricity generation in the form of wind-, solar- and hydropower are some of the popular sources of renewable energy.

Nuclear power, on the other hand, is more flexible, because it is a non-fossil, non-air-polluting and non-carbon emitting source of base-load energy supply. It can be used anywhere in the world and is not dependent on natural elements, like wind and water (necessary for wind- and hydro power) that is not freely available and accessible in most countries.

The most popular thermal reactors in operation today are LWRs (light water reactor), such as PWRs (pressurized water reactors) and BWRs (boiling water reactors), as well as the so-called heavy-water moderated reactors (CANDU). The first power station to utilise nuclear energy on an industrial scale to produce electricity was Calder Hall 1, which started operation in October 1956 and was decommissioned in March 2003 and is an advanced gas-cooled reactor [1]. A number of HTGRs (high temperature gas-cooled reactors) have been constructed and operated in Germany and the USA. Great interest has been demonstrated in the latter during the last number of years because of their intrinsic safety characteristics. Not only South Africa, but also China, Japan, South-Korea and the US are seriously considering this reactor type as future supply side energy source option.

The Pebble Bed Modular Reactor (PBMR) is a HTGR concept [2]. Reactor technologies, like the PWR, have the advantage of a long operational history with tried and tested tools and methods available for the analysis of the neutronics, thermal-hydraulics and transient states in the reactor. This has motivated the development of analysis tools and methods for HTGR for more accurate and efficient results.

During the development processes of new tools and methods, appropriate benchmarks will be defined and existing benchmarks used for the V&V (Verification and Validation) of existing and the updated version of the current computer code, TINTE (Time Dependant Neutronics and Temperatures) (Reitsma *et al.*, 2007:14) .

The purpose of this study is to focus on the group structure and cross-section generation / representation methods by comparing multi-group energy dynamics code, MGT (Multi-group TINTE) to a two-group code (TINTE). The results must show the differences and relevance when using different cross-section generation methods and the 2, 4, 6 or 8 energy group structures.

In this study the OECD (Organization for Economic Cooperation and Development) benchmark, calculated with TINTE, will form the basis for performing a comparative study between TINTE and MGT code. This benchmark is based on the PBMR 400 MWth reactor design and therefore it will be relevant to the PBMR.

1.2 Background to TINTE

TINTE is a 2D computer code originally developed by the Institute for Reactor Safety and Technology (ISR) at KFA (Kernforschungsanlage), now known as Forschungszentrum, Jülich - within the group responsible for nuclear safety and high temperature reactor technology. It deals with the thermal- and nuclear transient activities of the primary circuit of high temperature gas reactors giving the mutual feedback effects in two-dimensional r-z – geometry (Gerwin *et al.*, 1989:1) with a fixed two-group energy model.

1.3 Background to Multi-Group TINTE (MGT)

MGT is a development of TINTE aimed at carrying out multi-group time dependent neutron diffusion calculations. MGT retained the same code structure as the TINTE code but includes a few extras. MGT allows up to 43 broad neutron energy groups. These neutron energies are then divided into groups according to the group structure applicable. The energy group distribution can be seen in Figure 1-1 - where a two-group structure is illustrated.

In MGT there are three alternative methods to generate the time- and mesh-dependent cross-sections, namely (Lauer, 2007:2):

- Internal spectrum code calculation
- Function approximation by table interpolations
- Polynomial fit function

The in-line spectrum calculations take the actual conditions (temperatures, leakages and xenon concentration) into account when the fine-group spectrum is calculated and used to collapse to

few-groups. The table representation makes use of the same spectrum calculation to prepare the tables, but use pre-determined conditions and variations in these conditions to set up a matrix of cross-section values. The table representation of cross-sections is generated around a selected reference condition and the steady state conditions are typically used as this reference condition. During the calculation the cross-section is determined by interpolation between the pre-calculated data based on the actual conditions at that time step.

In MGT there is a choice to use the above mentioned methods independently in the material zones of the core models.

According to Gerwin & Lauer (2007), if a highly reliable and precise answer is needed, the internal spectrum input sets can be used, whereas a lower computing time is demanded, function approximation by table interpolation can be used. As seen in Figure 1-2, Internal spectrum code calculations' CPU time increase rapidly with the increase of energy groups, whereas function approximation by table interpolation- and polynomial fit function's CPU time is less than internal spectrum calculations and do not increase that rapidly with increasing energy groups (Clifford, 2007: 39).

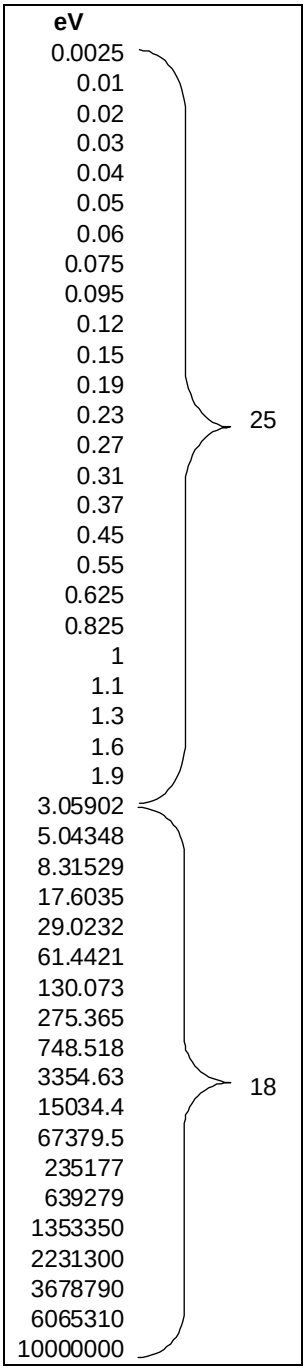

Figure 1-1: Neutron energies used in the energy group divisions in MGT, illustrated for a two-group structure

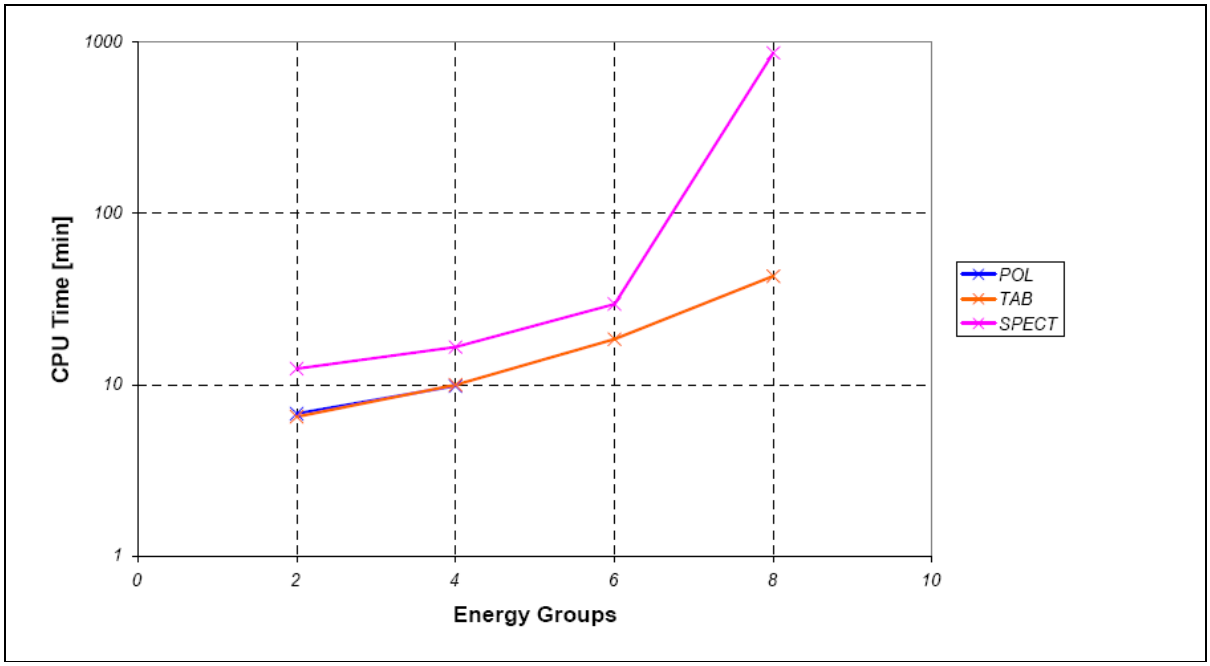

Figure 1-2: Internal spectrum code calculations' CPU time .

1.4 Similarities and difference between TINTE and MGT

The similarities and difference between TINTE and MGT that has been applicable to this study have been listed below.

Similarities:

- The same code system structure has been retained
- The classic TINTE reports and manuals are still used for MGT as well, except for the multi-group model

Differences:

- A new neutronic part has been developed in MGT to allow broad energy groups from 2 to 43 groups in contrast to only two fixed energy groups with TINTE
- Altered auxiliary routines to support multi-group neutronics
- Data post-processing routines have been modified and extended (and still compatible with TINTE)
- The tn4 file can be directly built up by the MInterf output files (tispec.inp and life.tn4) where the cross-section data base consists of material zones incorporated in the Tispec input file instead of the coefficients of the polynomial expansion series. The same reactor model can be used to create various tn4 files with only some/all material zones by using:

i. tabular
ii. polynomial X-S functions

- Each material zone can be specified individually from 5 different cross-section sets: (The broad energy groups just have to be the same for each material zone)
    i. Input sets for internal Tispec spectrum calculations
    ii. Tabulated data sets for linear cross-section interpolation
    iii. Coefficient sets for polynomial expansions of cross-sections
    iv. The same for the expansion, not of the X-S themselves, but for the square roots of them (to avoid negative fit values) and for the
    v. Logarithms of the X-S
- New program usage scripts for MGT – still analogous to TINTE, but start with the letter M (except for two scripts – HE and TPINT), for example MInterf, MGT (instead of TINTE)

1.5 Problem Statement

TINTE's original version (version 204d) only distinguishes between thermal and fast regions with a two-group polynomial method. A TINTE derivative has been developed, namely MGT which can perform up to 43-group calculations. The "OECD/NEA/NSC PBMR coupled neutronics/thermal hydraulics transient benchmark of the PBMR-400 core design" will be used for comparison. A special feature was added to this benchmark specification, to enable TINTE to read multi-dimensional cross-section tables (including cross-terms).

The emphasis will be placed on the influence of group structure and cross-section representation. More energy groups may be more accurate, but the calculation becomes much more expensive, hence a balance between accuracy and calculation effort must be found.

1.6 Purpose of the study

The purpose of this study is to evaluate the effects and importance of different cross-section representations and energy group structures for steady state and transient analysis and to determine a balance between accuracy and calculation effort.

Inputs and results received from PBMR (Pty) Ltd. were used to do the comparison.

A comparison will be made between two-group TINTE (OECD Benchmark) and the equivalent two energy groups and 4-, 6- and 8-groups in MGT to compare k-effective, as well as a study between 2, 4, 6 and 8 energy groups in MGT to investigate if the accuracy of a multi-group model with more than 4 energy groups improved. The characteristics that will be compared are fuel-, moderation- and maximum fuel temperatures, xenon concentration and k-effective.

The following codes were used to get the results (Clifford, 2008:8):

1. TINTE OECD build (compiled 2007/12/20), that uses the OECD benchmark cross-sections that were specified.
2. MGT beta version 0.91 that has the following limitations on the number of energy groups:
   - Inline spectrum calculations: 10 broad energy groups.
   - Tabulated cross-sections: 8 broad energy groups.
   - Polynomial cross-section expansions: 4 broad energy groups.

   In this version the original approximations of the non-local heat production of TINTE was kept unchanged. A new model, non-local heat deposition, with profiting of the possible finer fast energy group subdivision is not yet included in this model in order to use the multi-group model to its full potential (Clifford, 2008:9; Gerwin *& Lauer*, 2007:1).

The cross-section generation methods to be compared in this study are OECD Benchmark Tables, the inline spectrum- and tabulated cross-section method to compare up to 8 groups. Analysis in the case of the polynomial cross-section expansions representation is not available up to 8 groups and thus not included in the comparison.

1.7 Method of Approach

The OECD benchmark cases, calculated with TINTE, will form the basis for performing a comparative study between TINTE and MGT codes. Results from the MGT beta version 0.91, which were received from PBMR, will be used for the comparison.

Table 1-1: Description of cases to be compared

Case Nr	Steady state	Transient	Case Description	Group Structure				Usage
				2	*4*	*6*	*8*	*TINTE/MGT*
1	✓		Combined neutronics thermal hydraulics calculation – this is the starting condition for the transient calculations.	✓	✓	✓	✓	**TINTE (OECD Benchmark Tables) MGT ((table interpolation, internal spectrum)**
2		✓	Reactivity insertions by total control rod withdrawal.	✓	✓	✓	✓	**MGT (table interpolation, internal spectrum)**

1.8 Outline of the study

The next chapter describes the PBMR-cycle, OECD benchmark and discusses the simplifications introduced in the benchmark model. The OECD benchmark steady state and transient cases used in this study will be identified and their definitions will be given.

Chapter three will include a general multi-group terminology investigation, including LWR's, BWR's and CANDU reactor group structure. Previous studies on energy group structures will be discussed in this chapter.

In chapter four a steady state investigation will be discussed using the OECD benchmark steady state case 3. TINTE (2-group OECD Benchmark Tables) and MGT (2, 4, 6 and 8 energy groups - internal spectrum code calculations and function approximation by table interpolations) will be compared.

Chapter five will indicate the transient investigations. The OECD benchmark transient case 5a will be discussed. Characteristics that will be compared include the following: reactor power, moderator- and maximum fuel temperatures.

The study is finalised in chapter six with a conclusion and recommendations for future work.

1.9 Outcomes of this study

The following outcomes are needed to successfully complete this study:

- A literature survey to help define the terms "one-group", "two-groups" and "multi-groups".
- Identification of previous work done and current nuclear reactors' energy group structures.
- To do a comparative study between the two cross-section generation methods mentioned below, in conjunction with the group structures changing from 2, 4, 6 and 8 groups.
  - Internal spectrum code calculation.
  - Function approximation by table interpolations.
- To do an evaluation of the compared results and make the appropriate conclusions as to whether the use of a multi-group energy structure (especially more than 4 groups) is more accurate than a two-group structure and the influence of the
  - energy group structures; and
  - cross-section generation methods.

2. CHAPTER TWO: BACKGROUND

Make a commitment to commit yourself to achieving your goals
John Maxwell

2.1 Introduction

The background relating to the PBMR cycle and the "OECD/NEA/NSC PBMR coupled neutronics/thermal hydraulics transient benchmark of the PBMR-400 core design" will be discussed.

2.2 Review of PBMR cycle

The PBMR (Pty) Ltd. is a South African company that was established in 1999 and is situated in Centurion, Pretoria. PBMR is developing the Pebble Bed Modular Reactor which is a generation IV, high temperature, gas cooled reactor (HTGR) with a closed-cycle, gas turbine power conversion system, fueled with uranium dioxide (UO_2) and graphite moderated. Factors like the design, materials, fuel and physics all contribute to the intrinsic safety of the PBMR. The layout of the PBMR can be seen in Figure 2-1 (**Error! Reference source not found.**).

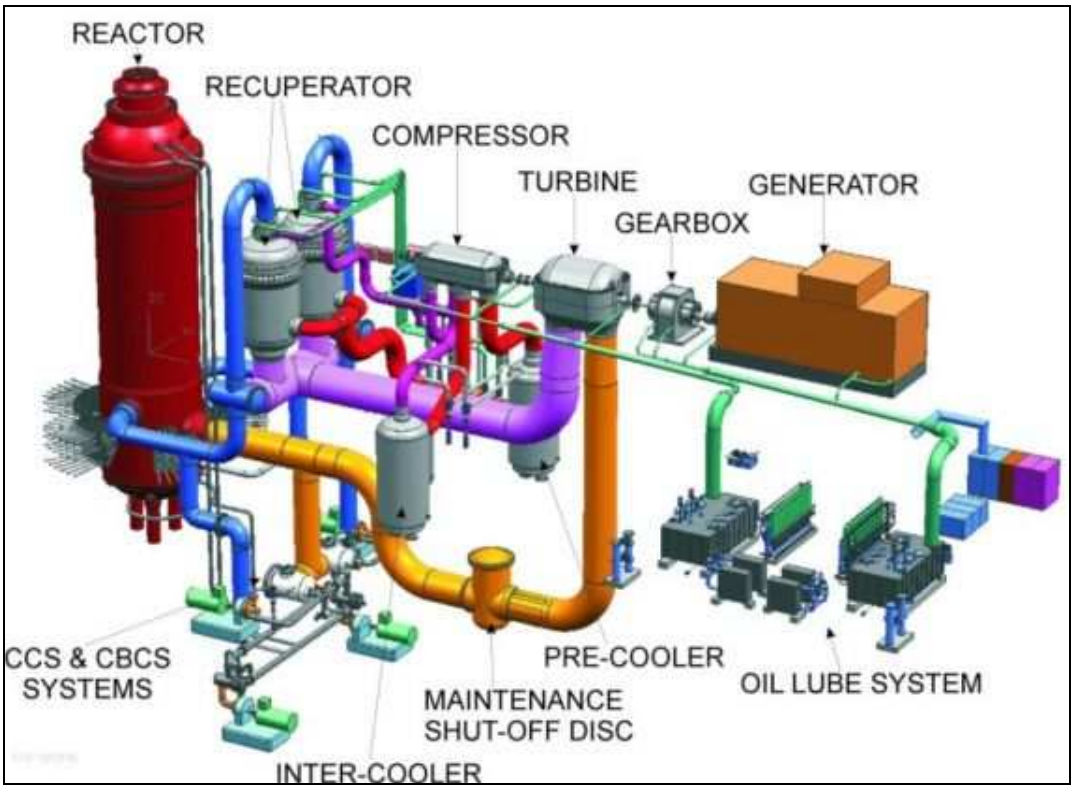

Figure 2-1: Layout of PBMR.

The 400MW PBMR (reactor unit and core layout can seen in Figure 2-2) is the reference core design (Reitsma *et al.*, 2007:18) and features an annular core layout with an inner- or central reflector, an outer- and inner diameter of 3.7 and 2 meters respectively, and an effective cylindrical core height of 11 meters. The side reflector (graphite) is approximately 90 centimeters thick.

There are three equi-speed fuel loading and -unloading tubes equi-spaced in the centre of the fuel annulus. During normal operation, 24 partial control rods (B_4C) that are positioned in the side reflector, operate together. The 24 control rods consist of 12 lower shutdown rods and 12 upper control rods, with an effective length of 6.5 meters. An additional shutdown system, the reserve shutdown system (RSS), positioned in the fixed central reflector, consists of eight small absorber sphere systems filled with 1 centimeter diameter absorber spheres containing a predetermined concentration of B_4C and graphite.

The reactor pressure vessel (RPV) has an inner diameter of 6.2 meter and is approximately 27 meter high. A 90 cm graphite-brick-lining serves as an outer reflector and a passive heat transfer medium.

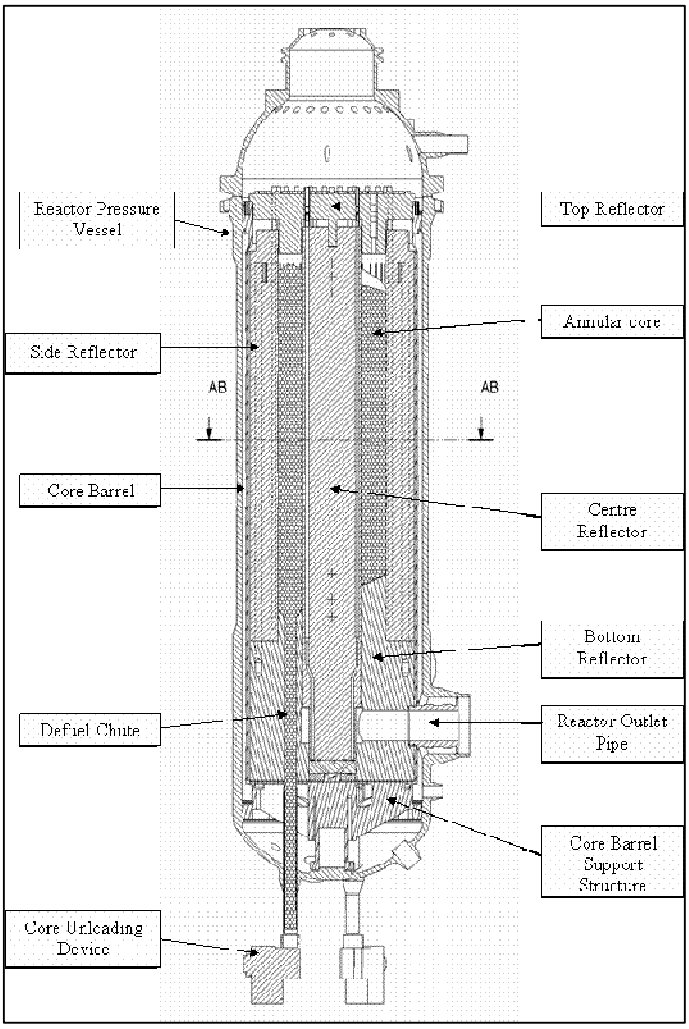

Figure 2-2: The PBMR 400MW reactor unit design (Reitsma *et al*, 2007:18).

Approximately 452,000 fuel pebbles fill the core with a packing fraction of 0.61 with an enrichment of 9.6wt% in the U-235 isotope. The inner 2.5cm radius of the pebble contains around 15,000 UO_2 TRISO-coated micro-spheres embedded in a graphite matrix. The coated particle acts as containment for the fission products produced. Figure 2-3 is a typical depiction of a fuel pebble.

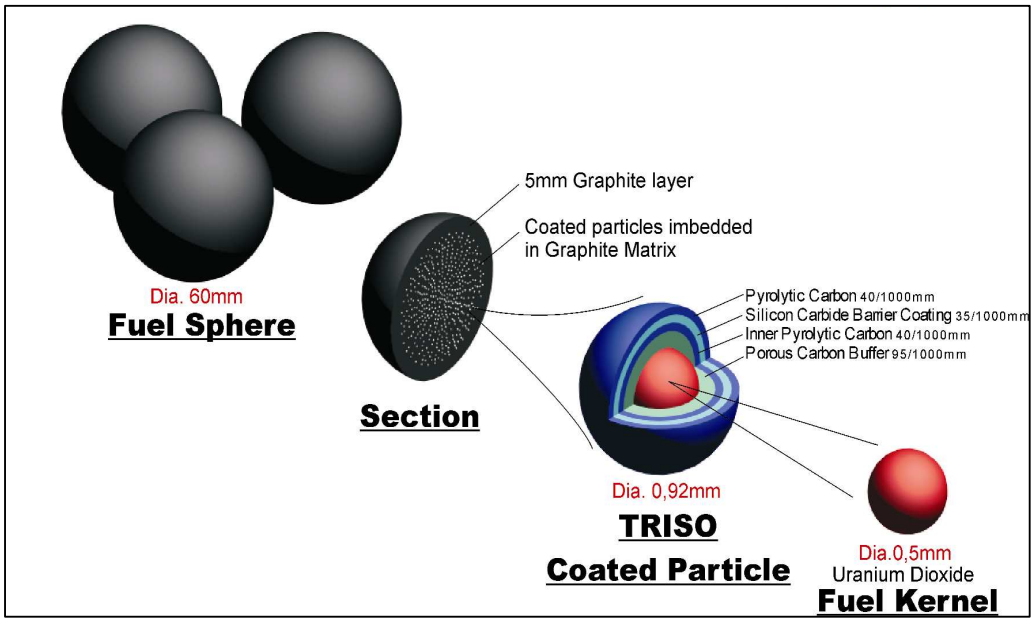

Figure 2-3: Graphical representation of the fuel pebbles [2]Error! Reference source not found.

2.3 Review of OECD benchmark

The Pebble Bed Modular Reactor coupled neutronics/thermal transient benchmark problem has been included by the Nuclear Energy Agency (NEA) of the Organization for Economic Cooperation and Development as part of their official activities (Gougar, 2006:10).

During the development processes of new tools and methods, appropriate benchmarks will be defined and existing benchmarks used for the V&V (verification and validation) of existing and the updated version of the current computer code, TINTE, (Reitsma *et al.*, 2007:14) .

The PBMR-400 benchmark problem is derived from the 400 MWth design of the demo unit. Simplifications are included in the design to limit approximations in the benchmark problem, but the important characteristics of the reactor still have to be preserved. These simplifications will ensure a mutual representative design for accurate and relevant results.

2.3.1 *Simplifications introduced in benchmark model*

Specific simplifications were introduced into the benchmark problem to limit the need for approximations in the model (Reitsma *et al.*, 2007:19).

2.3.1.1. Core design simplifications

All the simplifications in the core design make the core two-dimensional, in (r,z) geometry. These simplifications include the following:

- Flat bottom reflector by flattening the pebble bed's upper surface and the removal of the bottom core en de-fuelling channel.
- Parallel flow channels at equal speeds.

2.3.1.2. Thermal-hydraulic simplifications

Thermal-hydraulic simplifications include:

- No mass flow between the reactor pressure vessel and barrel and the side reflector and barrel.
- No mass flow between the reactor pressure vessel and the outer boundary.
- Coolant flow is defined through the main engineering flow paths: upwards flow through a porous annulus in the side reflector, downwards flow through the pebble bed to the outer plenum.
- No reflector cooling or leakages were defined.
- The cooling dowels and slits were ignored as well as the 10cm diater hole in the middle of the central reflector.

The assumption that the heat sources from fission will be deposited locally was made. In other words, no other heat sources exist outside the core. This was balanced by the effect of excluding bypass flows.

2.3.1.3. Core Geometry and dimensions

Figure 2-4 shows half of the reactor (with a symmetry axis on the zero radius in the middle of the reactor.) The material mesh dimensions can be seen in in the (r,z) direction.

The material regions representation can be seen in the core layout definition below. More detail on the dimensions can be seen in Table 2-1.

	0	10	41	73.6	80.55	92.05	100	117	134	151	168	185	192.95	204.45	211.4	225	243.6	260.6	275	287.5	292.5	310	328	462	463
-235		10	31	32.6	6.95	11.5	7.95	17	17	17	17	17	7.95	11.5	6.95	13.6	18.6	17	14.4	12.5	5	17.5	18	134	1
-200	35	TP	TP	TP	TP	TP	TP	TP	TP	TP	TP	TP	TP	TP	TP	TP	TP	TP	TP	TP	TP	He	RPV	Air	RCCS
-150	50	CC	CC	CC	CC	RSS	CC	TR	TR	TR	TR	TR	SR	RCS	SR	SR	SR	SR	SR	He	CB	He	RPV	Air	RCCS
-100	50	CC	CC	CC	CC	RSS	CC	TR	TR	TR	TR	TR	SR	RCS	SR	SR	SR	SR	SR	He	CB	He	RPV	Air	RCCS
-50	50	CC	CC	CC	CC	RSS	CC	TR	TR	TR	TR	TR	SR	RCS	SR	SR	SR	SR	SR	He	CB	He	RPV	Air	RCCS
0	50	CC	CC	CC	CC	RSS	CC	V	V	V	V	V	SR	RCS	SR	SR	SR	SR	SR	He	CB	He	RPV	Air	RCCS
50	50	CC	CC	CC	CC	RSS	CC	F	F	F	F	F	IP	RCS	IP	IP	IP	RC	SR	He	CB	He	RPV	Air	RCCS
100	50	CC	CC	CC	CC	RSS	CC	F	F	F	F	F	SR	RCS	SR	SR	SR	RC	SR	He	CB	He	RPV	Air	RCCS
150	50	CC	CC	CC	CC	RSS	CC	F	F	F	F	F	SR	RCS	SR	SR	SR	RC	SR	He	CB	He	RPV	Air	RCCS
200	50	CC	CC	CC	CC	RSS	CC	F	F	F	F	F	SR	RCS	SR	SR	SR	RC	SR	He	CB	He	RPV	Air	RCCS
250	50	CC	CC	CC	CC	RSS	CC	F	F	F	F	F	SR	RCS	SR	SR	SR	RC	SR	He	CB	He	RPV	Air	RCCS
300	50	CC	CC	CC	CC	RSS	CC	F	F	F	F	F	SR	RCS	SR	SR	SR	RC	SR	He	CB	He	RPV	Air	RCCS
350	50	CC	CC	CC	CC	RSS	CC	F	F	F	F	F	SR	RCS	SR	SR	SR	RC	SR	He	CB	He	RPV	Air	RCCS
400	50	CC	CC	CC	CC	RSS	CC	F	F	F	F	F	SR	RCS	SR	SR	SR	RC	SR	He	CB	He	RPV	Air	RCCS
450	50	CC	CC	CC	CC	RSS	CC	F	F	F	F	F	SR	RCS	SR	SR	SR	RC	SR	He	CB	He	RPV	Air	RCCS
500	50	CC	CC	CC	CC	RSS	CC	F	F	F	F	F	SR	RCS	SR	SR	SR	RC	SR	He	CB	He	RPV	Air	RCCS
550	50	CC	CC	CC	CC	RSS	CC	F	F	F	F	F	SR	RCS	SR	SR	SR	RC	SR	He	CB	He	RPV	Air	RCCS
600	50	CC	CC	CC	CC	RSS	CC	F	F	F	F	F	SR	RCS	SR	SR	SR	RC	SR	He	CB	He	RPV	Air	RCCS
650	50	CC	CC	CC	CC	RSS	CC	F	F	F	F	F	SR	RCS	SR	SR	SR	RC	SR	He	CB	He	RPV	Air	RCCS
700	50	CC	CC	CC	CC	RSS	CC	F	F	F	F	F	SR	RCS	SR	SR	SR	RC	SR	He	CB	He	RPV	Air	RCCS
750	50	CC	CC	CC	CC	RSS	CC	F	F	F	F	F	SR	RCS	SR	SR	SR	RC	SR	He	CB	He	RPV	Air	RCCS
800	50	CC	CC	CC	CC	RSS	CC	F	F	F	F	F	SR	RCS	SR	SR	SR	RC	SR	He	CB	He	RPV	Air	RCCS
850	50	CC	CC	CC	CC	RSS	CC	F	F	F	F	F	SR	RCS	SR	SR	SR	RC	SR	He	CB	He	RPV	Air	RCCS
900	50	CC	CC	CC	CC	RSS	CC	F	F	F	F	F	SR	RCS	SR	SR	SR	RC	SR	He	CB	He	RPV	Air	RCCS
950	50	CC	CC	CC	CC	RSS	CC	F	F	F	F	F	SR	RCS	SR	SR	SR	RC	SR	He	CB	He	RPV	Air	RCCS
1000	50	CC	CC	CC	CC	RSS	CC	F	F	F	F	F	SR	RCS	SR	SR	SR	RC	SR	He	CB	He	RPV	Air	RCCS
1050	50	CC	CC	CC	CC	RSS	CC	F	F	F	F	F	SR	RCS	SR	SR	SR	RC	SR	He	CB	He	RPV	Air	RCCS
1100	50	CC	CC	CC	CC	RSS	CC	F	F	F	F	F	SR	RCS	SR	SR	SR	RC	SR	He	CB	He	RPV	Air	RCCS
1150	50	CC	CC	CC	CC	RSS	CC	BR	BR	BR	BR	BR	SR	RCS	SR	SR	SR	RC	SR	He	CB	He	RPV	Air	RCCS
1200	50	CC	CC	CC	CC	RSS	CC	BR	BR	BR	BR	BR	SR	RCS	SR	SR	SR	RC	SR	He	CB	He	RPV	Air	RCCS
1250	50	CC	CC	CC	CC	RSS	CC	BR	BR	BR	BR	BR	SR	RCS	SR	SR	SR	RC	SR	He	CB	He	RPV	Air	RCCS
1300	50	CC	CC	CC	CC	CC	CC	BR	BR	BR	BR	BR	SR	SR	SR	SR	SR	IP	SR	He	CB	He	RPV	Air	RCCS
1350	50	CC	CC	CC	CC	CC	CC	BR	BR	BR	BR	BR	SR	SR	SR	SR	SR	SR	SR	He	CB	He	RPV	Air	RCCS
1400	50	CC	CC	CC	CC	CC	CC	OP	OP	OP	OP	OP	SR	SR	SR	SR	SR	SR	SR	He	CB	He	RPV	Air	RCCS
1450	50	CC	CC	CC	CC	CC	CC	BR	BR	BR	BR	BR	SR	SR	SR	SR	SR	SR	SR	He	CB	He	RPV	Air	RCCS
1500	50	CC	CC	CC	CC	CC	CC	BR	BR	BR	BR	BR	SR	SR	SR	SR	SR	SR	SR	He	CB	He	RPV	Air	RCCS
1535	35	BP	BP	BP	BP	BP	BP	BP	BP	BP	BP	BP	BP	BP	BP	BP	BP	BP	BP	BP	BP	He	RPV	Air	RCCS

CORE LAYOUT DEFINITIONS

F	REACTOR CORE CONTAINING THE FUEL
V	HELIUM GAP BETWEEN FUEL AND TOP REFLECTOR: VOID
CC	CENTRAL REFLECTOR: GRAPHITE
TR	TOP REFLECTOR: GRAPHITE
BR	BOTTOM REFLECTOR: GRAPHITE
SR	SIDE REFLECTOR: GRAPHITE
RCS	REACTOR CONTROL SYSTEM CHANNEL : GRAPHITE / GREY CURTAIN AREA
RSS	RESERVE SHUTDOWN SYSTEM CHANNEL : GRAPHITE / GREY CURTAIN AREA
IP	INLET PLENUM TOP / BOTTOM : GRAPHITE
RC	RISER CHANNEL IN SIDE REFLECTOR : GRAPHITE
OP	OUTLET PLENUM BOTTOM : GRAPHITE
He	STAGNANT HELIUM
TP	TOP PLATE : IRON : ADIABATIC BOUNDARY
BP	BOTTOM PLATE : IRON : ADIABATIC BOUNDARY
CB	CORE BARREL : IRON
RPV	REACTOR PRESSURE VESSEL : IRON
Air	STAGNANT AIR
RCCS	REACTOR CAVITY COOLING SYSTEM : 20C TH BOUNDARY
	NEUTRONIC BOUNDARY CONDITIONS

Figure 2-4: Core geometry of PBMR-400 benchmark model (Reitsma *et al.*, 2007:21).

Table 2-1: Core geometrical specifications at room temperature (Reitsma *et al.*, 2007:22).

	Description	Unit	Value
1.	Equivalent core outer radius.	m	1.85
2.	Cylindrical height of the core (flattened core surface at the top and flat bottom reflector).	m	11.0
3.	Total core volume.	m^3	83.7155
4.	Fixed central column graphite reflector radius.	m	1.0
5.	Effective height of the upper void cavity (levelled core surface to bottom of top reflector).	m	0.5
6.	Effective annular thickness of the side reflector (graphite).	m	0.9
7.	Inner radius of the core barrel.	m	2.88
8.	The wall thickness of the core barrel.	m	0.05
9.	The inner radius of the RPV	m	3.1
10.	The wall thickness of the RPV.	m	0.18
11.	Radius of cooling system/20˚ C temperature isothermal boundary.	m	4.62
12.	Radii of five material meshes in core (5 radial material meshes in core, equal width).	m	1.17 1.34 1.51 1.68 1.85
13.	Thickness of core radial meshes (all equal).	m	0.17
14.	Axial material mesh: 11.0 m / 22 meshes (in core).	m	0.5
15.	Outlet plenum inner radius.	m	1.0
16.	Outlet plenum outer radius.	m	1.85
17.	Outlet plenum height.	m	0.5
18.	Inlet plenum inner radius.	m	2.436
19.	Inlet plenum outer radius.	m	2.606
20.	Inlet plenum height.	m	0.5
21.	He riser channel skirt / porous region inner radius.	m	2.436
22.	He riser channel skirt /porous region outer radius.	m	2.606
23.	Distance from bottom of core to top of the inlet plenum.	m	1.5
24.	Centre line axial distance between inlet and outlet plenum.	m	1.0
25.	Top inlet plenum inner radius.	m	1.85
26.	Top inlet plenum outer radius.	m	2.606
27.	Top inlet plenum height.	m	0.5
28.	Distance from bottom of top reflector to bottom of top inlet plenum (in the side reflector).	m	1.0
29.	Total height of top reflector.	m	1.5
30.	Total height of bottom reflector (distance from top of bottom plate to bottom of core).	m	4.0
31.	Top steel plate thickness.	m	0.35
32.	Bottom steel plate thickness.	m	0.35

2.3.1.4. Cross-sections

Cross-section changes of the PBMR-400 benchmark model (Reitsma *et al.*, 2007:28) that are due to the changes in the reactor are represented by the five-dimensional tables. The SPECTRUM code was used to generate cross-section sets for the following parameters and combinations thereof:

- Fuel temperature.
- Moderator temperature.
- Fast buckling.
- Thermal buckling.
- Xenon concentration.

A two-group energy structure was used with the cut-off energy of 3.059 eV (Reitsma *et al.*, 2007:28).

2.4 OECD benchmark case definitions

2.4.1 *Steady state benchmark*

Combined neutronics thermal hydraulics calculation - starting condition for the transients of the PBMR coupled neutronics/thermal hydraulics transient benchmark - the PBMR-400 core design (Reitsma et al., 2007:45) makes use of neutronics model description with the following conditions:

- Cross-section interpolation routines and provided tabulated cross-section data should be implemented in the codes and used.
- Make use of state parameter dependent tabulated set of macroscopic cross-sections.
- Equilibrium xenon distribution to be calculated.
- Calculate the temperatures distribution, outlet temperature, pressure drop over the core and heat loss to the RCCS.
- A coupled neutronics thermal hydraulic calculation is done, with feedback.

2.4.2 *Transient benchmark*

A transient calculation occurs when value/s change/s over time, with the starting point given as the steady state calculation or the steady state restart file.

The control rod withdrawal (CRW) of the PBMR coupled neutronics/thermal hydraulics transient benchmark - the PBMR-400 core design - with initial steady state full power conditions where (Clifford, 2008: 27):

- the control rods (CR) are at 202cm
- then the CR are withdrawn over a period of 5 second to 190 cm and
- then left to run up to 495 seconds.

A reasonably quick change in temperature and reactivity can occur when a CR withdrawal case is considered (Clifford, 2008:10). This case should also show significant spectral changes (different fine-group fluxes used to collapse the fine group cross-section to few-group cross-sections (weighting function)) and changed scattering properties of moderators and resonance absorptions (due to temperature changes) that changes the few-group macroscopic cross-sections used in the diffusion solution. Thus it is therefore sensitive to the method of cross-section preparation and group structure representation. The latter explains why these cases were being used.

3. CHAPTER THREE: LITERATURE SURVEY

Great people are ordinary people with an extraordinary amount of determination.
John Maxwell

3.1 Introduction

The main focus of this chapter is to define the terms "one-group", "two-groups" and "multi-groups". An investigation into the different group structures used in different reactors will also be done.

Reactor core physics calculations consist of two sets of calculations (Kriangchaiporn, 2006:1):

- To calculate the group cross-sections of the nuclear reactor.
- Using these cross-sections calculated by various methods to calculate the neutron distribution in order to investigate the reactor core.

3.1.1 *Two-group and multi-group definitions*

3.1.1.1. One-group theory:

One neutron energy spectrum covered by one energy group segment, for example from 0.025ev up to 10Mev consists of one energy group.

When straightforward geometries are used and steady state problems are solved numerically and analytically, a one-group reactor model is set up.

3.1.1.2. Two-group theory:

The neutron energy spectrum for a two-group model can be divided into two groups and consists of the following (also refer to Figure 3-1), (Rouben, 2008:3):

- Group 1: This can be described as the fast Group (or the slowing down groups).
- Group 2: This can be described as the thermal group.

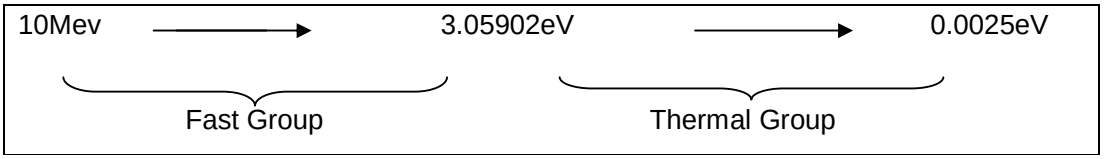

Figure 3-1: Two-group energy distribution.

The energy boundary (cut-off energy) separating the fast and the thermal groups in Figure 3-1, can be seen as 3.05902 eV.

3.1.1.3. Multi-group theory:

When the neutron energy spectrum is divided into more than 2 segments, it is a multi-group model. As the number of groups in the model increase, each segment's partition becomes smaller and smaller.

Figure 3-2: A 4-group (multi-group) energy distribution.

As Bernard (2006:1) stated that: "It has been found that a model using three or four groups, provides a very good representation of a thermal reactor. This is because most of the important neutron interactions take place at energies below 1 eV. For fast reactors, however, twenty or thirty groups are often necessary."

3.1.1.4. Few-Group theory:

If a group diffusion equation is averaged over portions of the spectra and it has a randomly assumed shape, it is called a multi-group equation. When parameters for group equations are originated by taking the average across the spectra to determine each material composition by a separate, infinite medium, a multi-group calculation can be named a few-group diffusion equations.

In other words, a multi-group model's spectra are assumed to be identified beforehand and is taken to be similar for all material compositions, whereas for a few-group calculation, a separate spectrum must be calculated (example: a multi-group solution of the position-independent equation).

3.1.2 *Neutron Flux Spectra for Thermal and Fast Breeder Reactors*

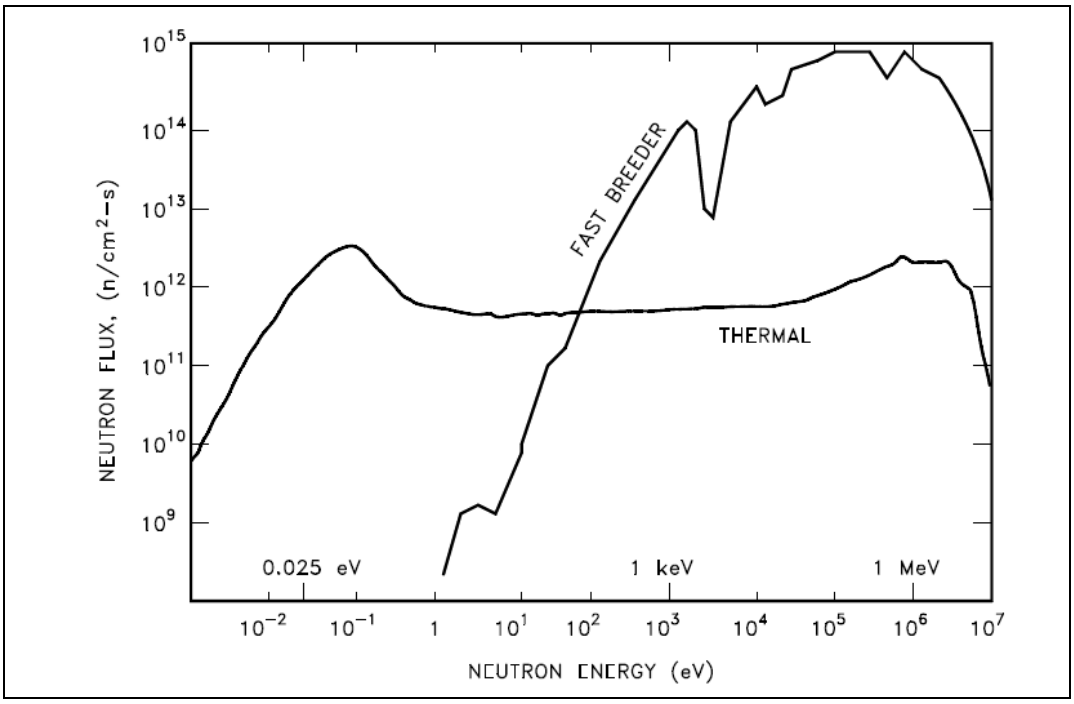

Figure 3-3: Neutron flux spectra for Fast Breeder – and Thermal Reactors

The neutron flux spectra of a thermal reactor differs from a fast breeder reactor, this can be seen in Figure 3-3. The reason for the different curve shapes can be attributed to the neutron slowing down (moderated) effects. For a thermal reactor (water or graphite moderated) a larger amount of neutrons exist at the lower energies, because of the following:

- In the intermediate region, from 1eV to 0.1 MeV, the flux in a thermal reactor has a 1/E dependence. (In other words, if the energy is halved, the flux doubles). This dependency is directly related to the slowing down effect. The neutron will lose more energy per collision at higher energies than at lower energies, thus the neutrons tend to “stack up” at this lower energies.

In the thermal region the neutrons will gain the energy it loses with consecutive collision when gaining and losing energy, within the distribution of energies, called the Maxwell distribution. (Nuclear Physics and Reactor Theory, 1993:34-35)

3.2 Why multi-group models?

The neutron energies encountered in a reactor typically span a range from 10^{-3} to 10^{7} eV. Neutron cross-sections are highly dependent on energy over most of this range. One-group models can hardly predict cross-sections accurately, because these can change in such a wide energy spectrum.

To give an illustration of the effect when using more than a one-group energy spectrum division, a simple cell model for a tank type experimental reactor is given in Figure 3-4 (Garland, 2005a:4-6).

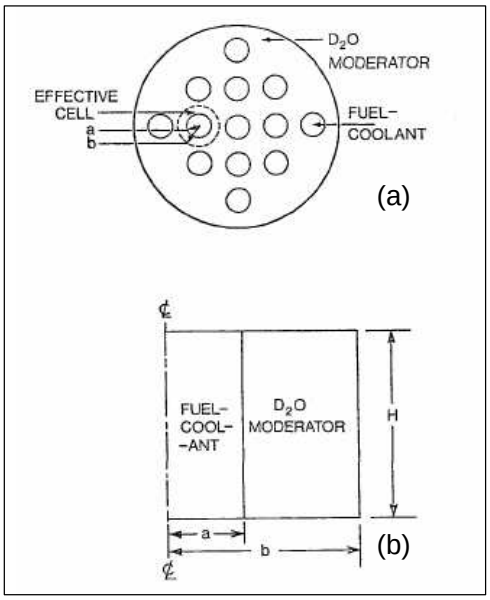

Figure 3-4: A schematic illustration of an experimental nuclear reactor model's (a) top view of the fuel bundles' lattice structure and (b) a side view of the two-region cell (Garland, 2005a:4).

In this study, criticality was achieved by varying the height of the D_2O moderator. By bubbling air through the coolant, a void formed. Again the height of the moderator was varied to maintain criticality. The experimental result - Buckling vs. void fraction is illustrated in Figure 3-5, compared to the calculated buckling.

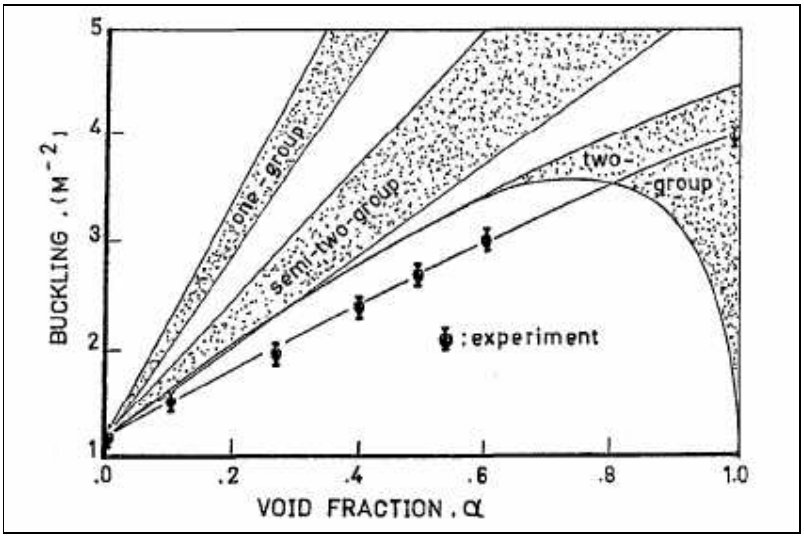

Figure 3-5: Experimental buckling vs. calculated buckling (Garland, 2005a:5).

As seen in Figure 3-5, the two-group theory's prediction of the buckling is the best. One group- and semi-two-group theory doesn't even come near the experimental values. In this case, 150 neutron energy groups are used to do the cell calculations to obtain the cell-averaged cross-sections. In order to get the full core calculation on this cell-averaged cross-section, few-group approximations are used. These few-group calculations can only be done accurately if it is based on detailed multi-group cell calculations (Garland, 2005a:6).

3.3 Previous work done on energy group structure

The PBMR 268 MWth benchmark was used as the source for this previous work (Tyobeka *et al.,* 2007:3).

The following simplifications were made to the 268 MWth design (Tyobeka *et al.*, 2007:3):

- Core design is two-dimensional (r-z) as seen in Figure 3-6.
- Flattening of the pebble-bed's upper surface.
- Removal of the bottom cone and the defuel channel - the outcome of this is a flat bottom reflector.
- Flow channels inside the pebble bed have been simplified to be parallel, while the pebbles travel at the same speed, and the central column and mixing zone widths were defined to remain constant over the total axial height.

- The control rods in the side reflector are modeled as a cylindrical skirt (2D) and are given a B-10 concentration.

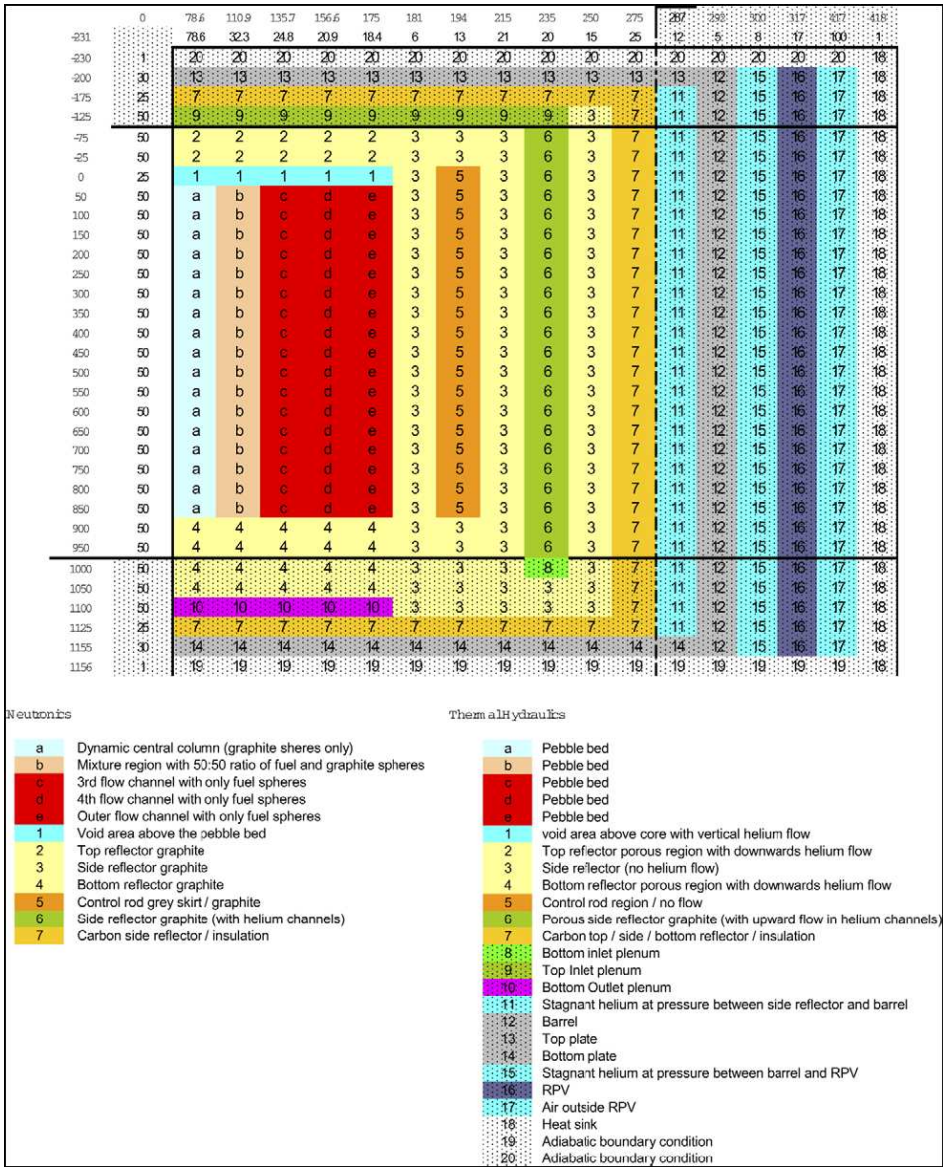

Figure 3-6: PBMR 268 MW_{th} core layout and material classification (Tyobeka *et al.*, 2007:3).

By using the DORT transport code (Johnson, 1992) three energy group structures were investigated, the cut-off points can be seen in the following paragraph for the 4, 7 and 13 group structures respectively (Tyobeka *et al.,* 2007:6):

4 group structure:

1.000E+07 → 1.11090E+05 → 2.90232E+01 → 2.38237E+00 → 0.00 (eV)

7 group structure:

1.000E+07 → 1.11090E+05 → 7.1017400E+03 → 2.90232E+01 → 2.38237E+00 → 1.85539E+00 → 0.0 (eV)

13 group structure:

1.000E+07 → 3.678E+06 → 1.11090E+05 → 7.1017400E+03 → 130.07 → 2.90232E+01 → 8.3153 → 2.38237E+00 → 1.85539E+00 → 0.625 → 0.200 → 0.075 → 0.0 (eV)

The group structures used in these calculations were motivated by the experience obtained from the following research reactors, AVR and THTR (Tyobeka *et al*., 2007:6).

In this study, the following was observed (Tyobeka et al., 2007:7):

- Using a large number of energy groups for transient studies in a coupled code is not plausible because of the dramatic increase in computational costs.
- The eigenvalue has a significant increase when changing from 4 energy groups up to 13 energy groups. As the number of energy groups increases, the difference in the eigenvalue increases. This can be seen in Table 3-1.
- The differences in power distribution are relative small. There are differences at the edges of the core, which can be explained by the treatment of the graphite reflector in the different energy groups (see Figure 3-2).

Table 3-1: Eigenvalue increase as the number of energy groups increase (Tyobeka *et al.*, 2007:6).

k_{eff} results for Case N2 (DORT studies on energy group structure)

Case	k_{eff} (rods partially inserted)	k_{eff} (rods fully inserted)	Differential CRW (pcm/cm)
4-energy groups	1.058310	0.922449	19.75
7-energy groups	1.058538	0.920801	20.02
13-energy groups	1.059697	0.917085	20.70

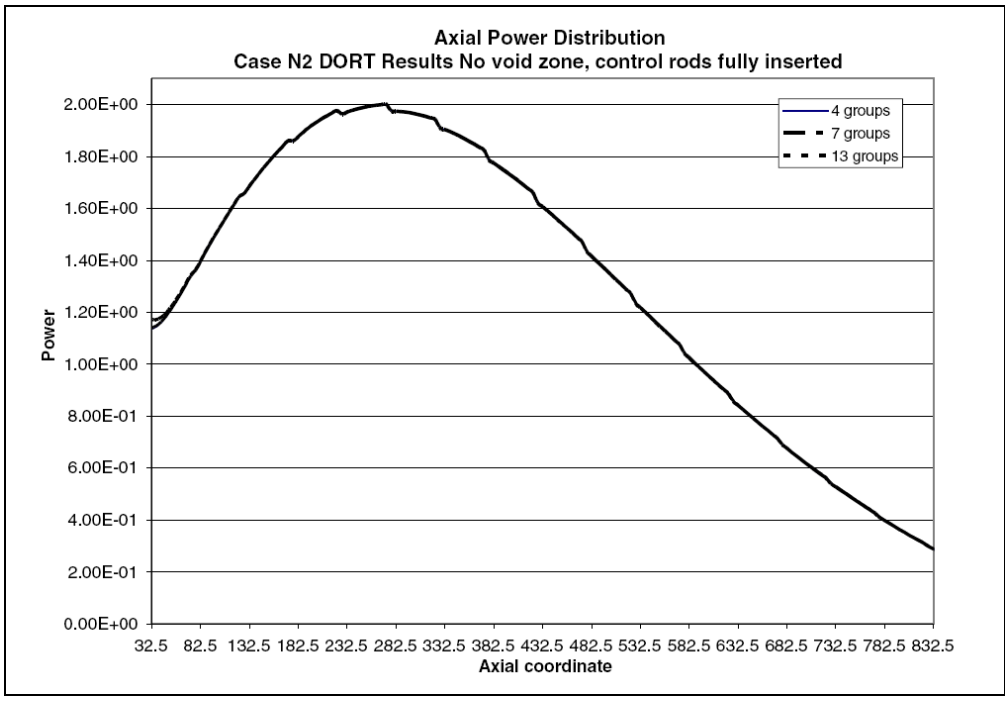

Figure 3-7: Axial power distribution presented as the number of energy groups increase (Tyobeka *et al.*, 2007:7).

3.4 Energy group structures of investigated and current nuclear reactors

3.4.1 *Introduction*

An investigation of energy group structures used in the industry and for research is indicated in the following paragraphs. A commercial type Light Water Reactor including example of pressurized water reactor (PWR) 1.16 GWe, the current Pebble Bed Modular Reactor (PBMR) design, HTR Modul 200, VHTR-600 and a CANada Deuterium Uranium (CANDU) reactor's group structure are illustrated and described.

3.4.2 *Light water reactors (LWR)*

The energy group structure of a LWR is divided into 2-groups:

1E+07 → 0.68256 → 1E-05 (eV)

Fast Group Thermal Group

3.4.2.1. PWR commercial type four loop 1.16 GWe reactor

The SRAC cross-section code library (Nakagawa & Mori, 1992:3) were used in the preparation of a 107 energy group library, that was collapsed into 4 energy groups with the energy boundaries (Nakagawa *& Mori,* 1992:3) as follows:

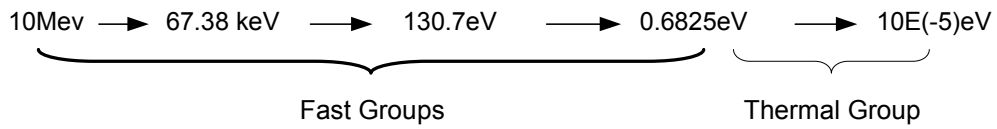

3.4.3 *Current PBMR Design*

The Very Superior Old Programs (VSOP) energy group structure (Stoker *et al*.) of the PBMR is divided into 4 energy groups with the following energy ranges (four groups were found to be good enough):

Thermal group	:	0 – 1.86 eV
Epithermal group	:	1.86 - 29 eV
		29 eV – 0.1 MeV
Fast group	:	0.1 MeV – 10 MeV

3.4.4 *VHTR 300 and VHTR 600*

The cross-sections for the fuel- and moderator materials were divided into six energy groups (Gougar *et al.*, 2004:267 and 273).

Thermal group	:	0 - 1.8554
		1.8554– 2.3823 eV
Epithermal group	:	2.3823 – 29.023 eV
		29.023 eV – 1.1109E5 eV eV
Fast group	:	1.1109E5 eV –1.6905E7 MeV

3.4.5 *CANDU Reactor*

With regard to the CANada Deuterium Uranium (CANDU) reactor XingGuan *et al.* (s.a.) state the following: "Experience has shown that there is no advantage in performing finite core analyses of the heavy-water-moderated CANDU in more than 2 energy groups. The use of 2 energy groups has made it possible to model the core accurately in 3 dimensions."

3.5 Conclusion

Only two energy groups can accurately model CANDU reactor (XingGuan *et al.*, s.a.:3), and for other thermal reactors a model using three to four groups gives a good representation of the reactor (Bernard, 2006). Will there be a remarkable gain by using more than a 2-group energy structure?

As was seen in section 3.3, according to Tyobeka *et al.* (2007), different energy group structures from 4- to 13 groups can cause a difference in the results. What influence will a 2, 4, 6 and 8 group structure have on the results?

As Gougar *et al.* (2004:104) state: "The cross-section libraries themselves may contribute to large differences." What will the effects be when the cross-sections are generated with the following two methods?

- Internal spectrum code calculation.
- Function approximation by table interpolations.

Chapter four will further investigate and expand on these effects.

4. CHAPTER FOUR: STEADY STATE INVESTIGATIONS

Success is achieved and maintained by those who keep trying.
John Maxwell

4.1 Introduction

In MGT, there are three alternative methods to generate the time- and mesh-dependent cross-sections, namely (Lauer, 2007:2):

- Internal spectrum code calculation.
- Function approximation by table interpolations.
- Polynomial fit function.

To compare the steady state case, the MGT 2-group calculations cross-section generation methods are as follows:

- internal spectrum code calculations method and
- function approximation by table interpolations were used to calculate the cross-sections

in comparison to the OECD benchmark Tables method in the TINTE 2-group calculation.

A 2, 4, 6 and 8 group comparison were done to investigate whether there will be a remarkable gain when using more than 2 energy groups in the calculations and to show the influence in results when using 2 methods for cross-section generation and multi-group energy structure. The balance between accuracy and calculation effort must be found in the number of energy groups used or the cross-section generation method.

A discussion of the steady-state case was presented in section 2.4.1.

Characteristics to be compared include the following: fuel-, core average-, moderation- and maximum fuel temperatures, xenon concentration and k-effective.

The energy structures of the steady state case can be illustrated as follows:

- 2 group energy structure:

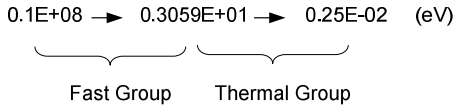

This group structure corresponds approximately with the VSOP energy group structure in 3.4.3 (Stoker *et al*.).

- 4 group energy structure:

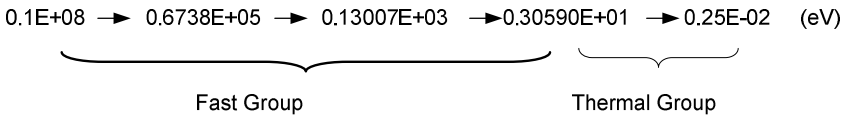

- 6 group energy structure:

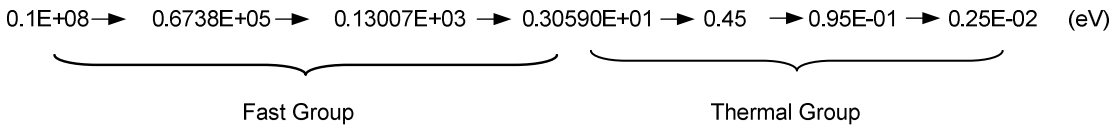

- 8 group energy structure:

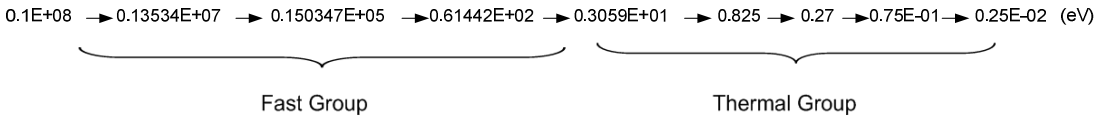

4.2 Results

4.2.1 *K-Effective Eigenvalues*

In Table 4-1 a comparison of the eigenvalues generated by using the internal spectrum- and table interpolation cross-section generation methods for 2-, 4-, 6- and 8 energy groups to the 2-group TINTE eigenvalue generated by the OECD Benchmark Tables. This was done to show, as expected, that a 8-group model is more accurate, when comparing it to the 2-group TINTE OECD Benchmark case.

Table 4-1: Eigenvalues in comparison to the eigenvalue generated by the 2-group TINTE OECD Benchmark Tables.

Case	K-eff	Difference in eigenvalue in respect to 2-group TINTE OECD (*pcm)
2-group TINTE_OECD	0.99366	0
2-group Internal Spectrum	1.00161	+795
2-group Table Interpolation	1.00263	+897
4-group Internal Spectrum	0.98907	-459
4-group Table Interpolation	0.98961	-405
6-group Internal Spectrum	0.99059	-307
6-group Table Interpolation	0.99035	-331
8-group Internal Spectrum	0.99180	-186
8-group Table Interpolation	0.99137	-229

* pcm = 1E-5

From Table 4-1 it can be seen that the finer the energy-group structure, the closer the results are in comparison to the 2-group TINTE OECD results. According to Gerwin *& Lauer* (2007), if a highly reliable and precise answer is needed, the internal spectrum input sets can be used, whereas a lower computing time is demanded, function approximation by table interpolation can be used.

The 43 pcm differences in the K-eff of the Internal Spectrum and Table Interpolation 8-group calculations are accepted as insignificant. Therefore the reference for this study comparison is chosen as the 8-group Internal Spectrum set.

Table representation is also expected to perform well (precise) at steady state condition since the steady state conditions (actual conditions at that step) are typically used to calculate the cross-sections and therefore no interplation is needed. This is

achieved by rerunning the Spectrum precalculation with the TINTE/MGT conditions as input for a few iterations.

Table 4-2: Eigenvalues of 2, 4, 6 and 8 steady state groups by using the internal spectrum and table interpolation cross-section generation methods

Case	K-eff	Difference in eigenvalue in respect to 8-group Internal Spectrum (*pcm)
2-group Internal Spectrum	1.00161	981
4-group Internal Spectrum	0.98907	-273
6-group Internal Spectrum	0.99059	-121
8-group Internal Spectrum	**0.9918	0
2-group Table Interpolation	1.00263	1083
4-group Table Interpolation	0.98961	-219
6-group Table Interpolation	0.99035	-145
8-group Table Interpolation	0.99137	-43

* pcm = 1E-5

** Taken as Calculational Reference

4.2.2 *Internal spectrum calculation comparison*

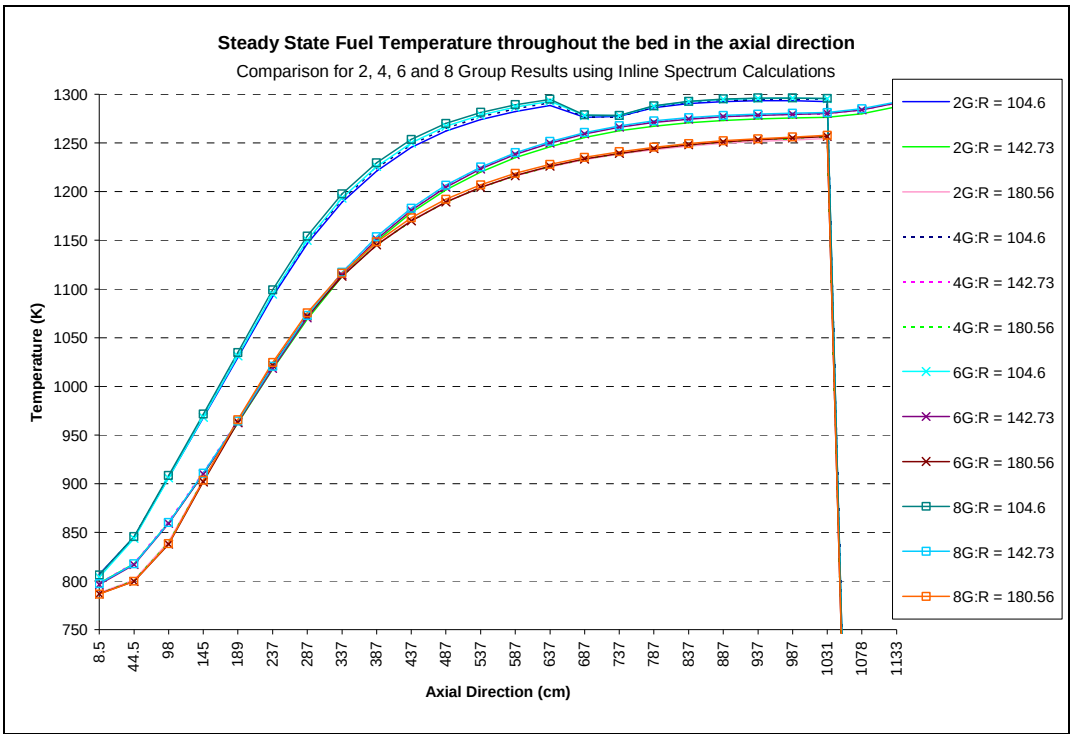

Figure 4-1: The fuel temperature throughout the bed in the axial direction using the inline spectrum calculation method.

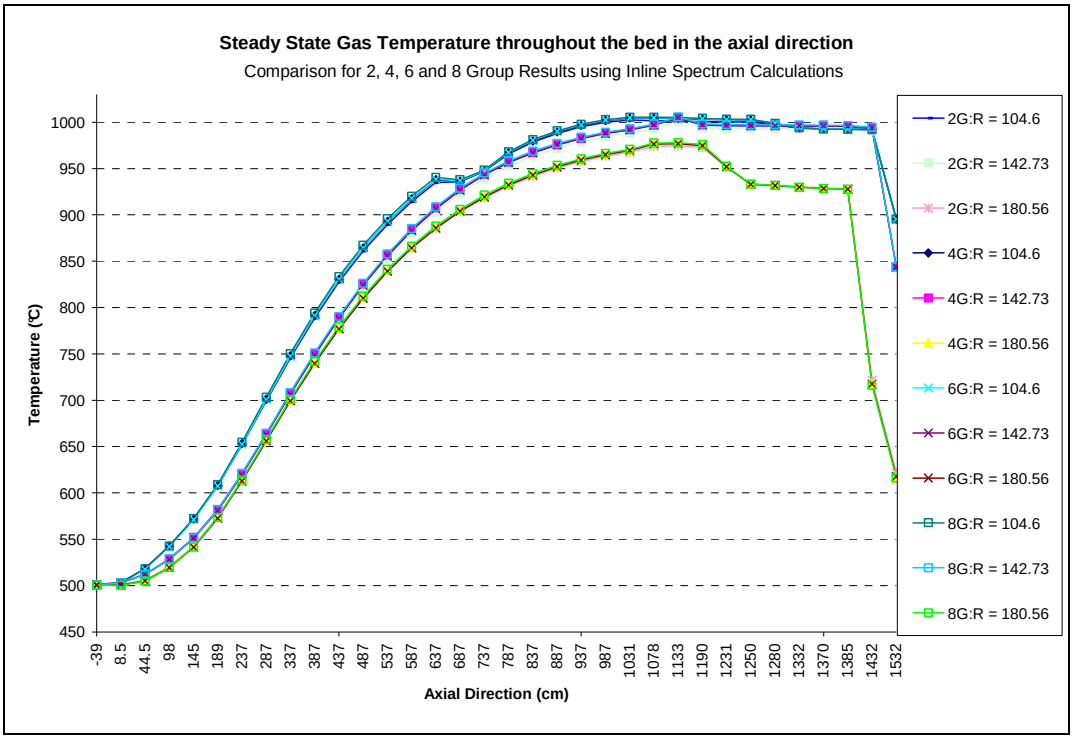

Figure 4-2: The gas temperature throughout the bed in the axial direction using the inline spectrum calculation method.

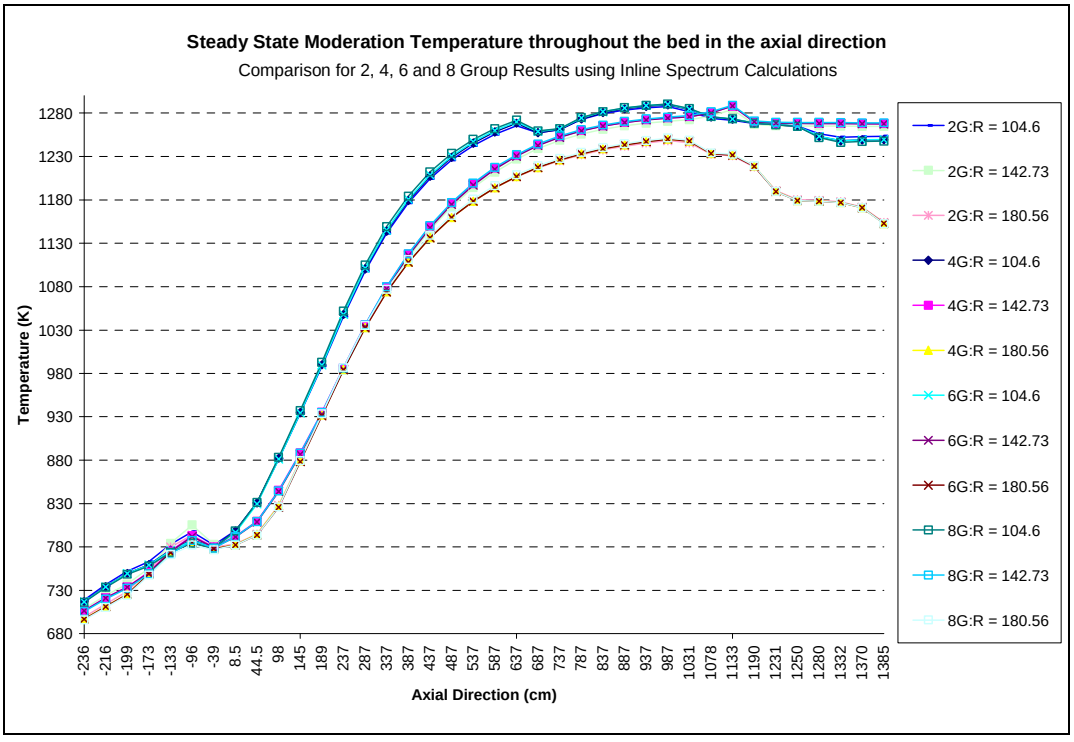

Figure 4-3: The moderation temperature throughout the bed in the axial direction using the inline spectrum calculation method

4.2.3 *Function approximation by table interpolation calculation comparisons*

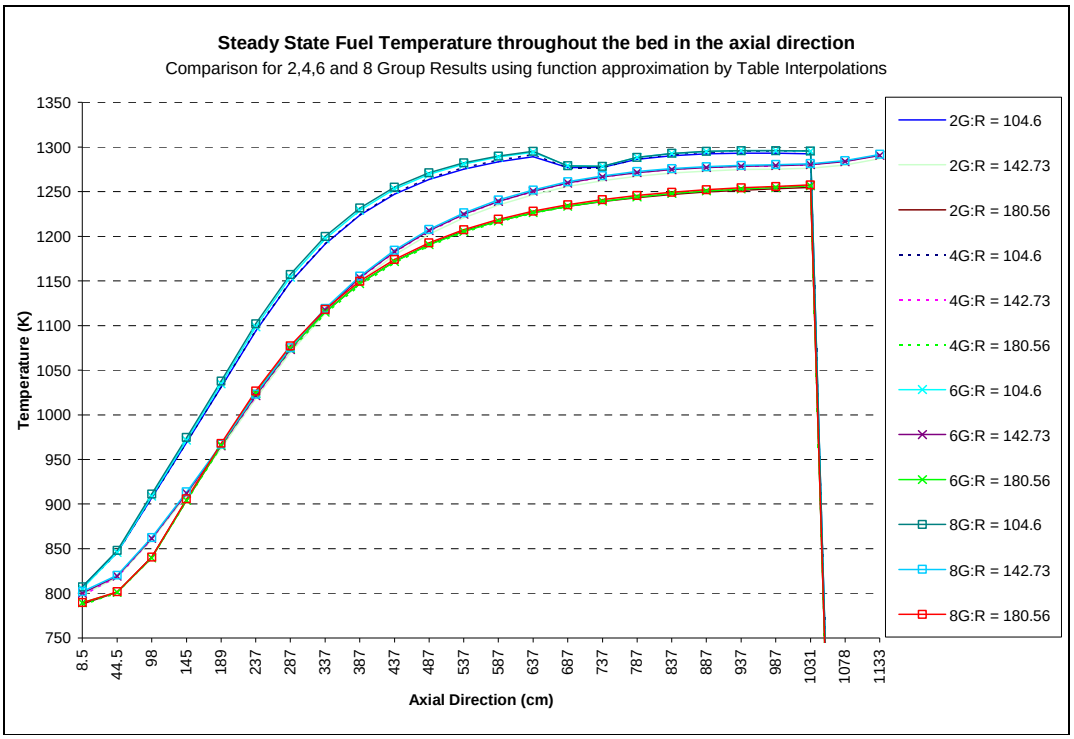

Figure 4-4: The fuel temperature throughout the bed in the axial direction using the function approximation by table interpolation method.

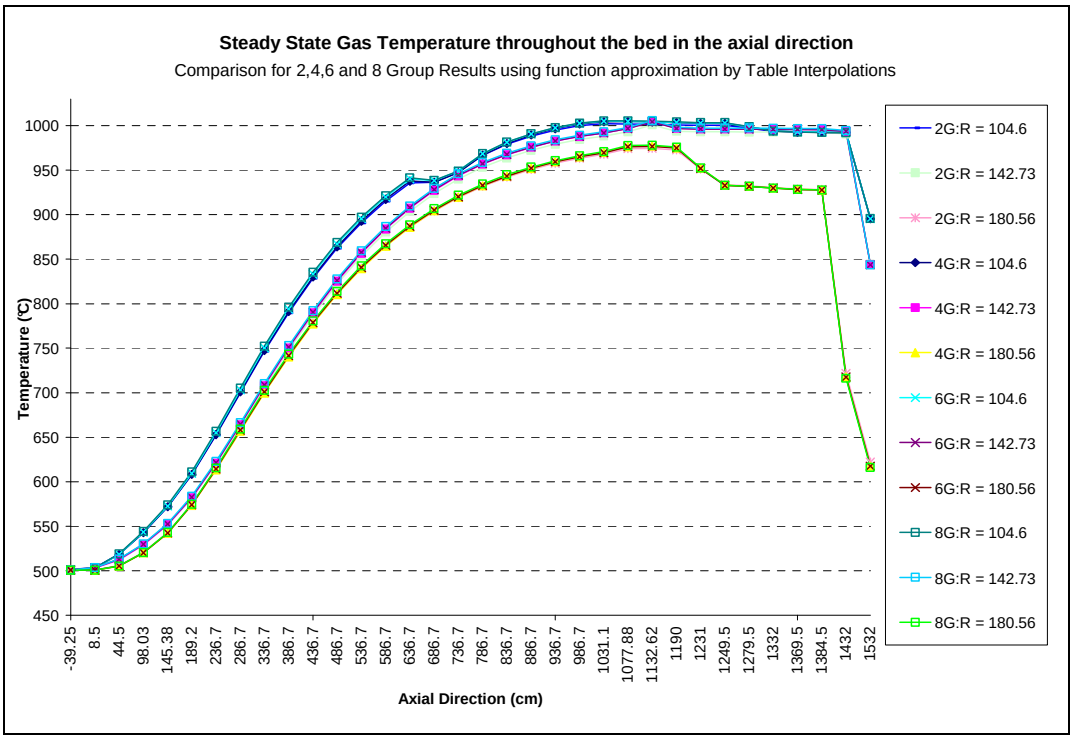

Figure 4-5: The gas temperature throughout the bed in the axial direction using the function approximation by table interpolation method.

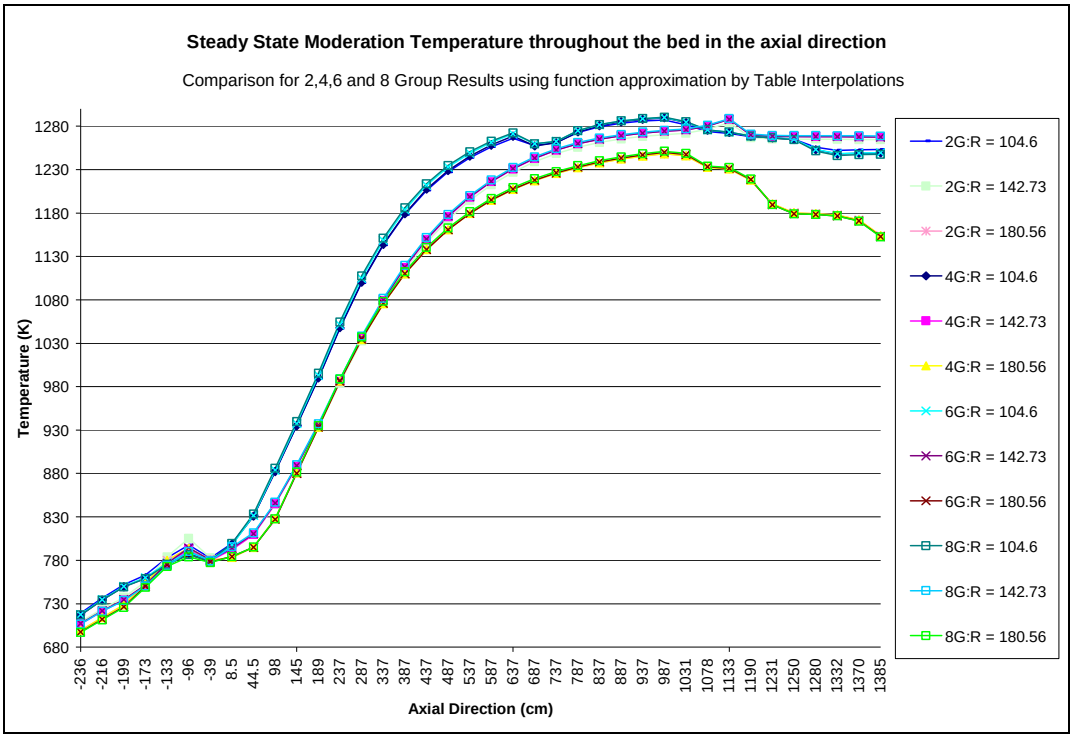

Figure 4-6: The moderation temperature throughout the bed in the axial direction using the function approximation by table interpolation method.

Samples from Figure 4-1 to Figure 4-6 were considered at the following positions:

- Fuel temperature: Radial 104.6 cm and axial 536.7 cm.
- Gas temperature: Radial 104.6 cm and axial 986.7 cm.
- Moderation temperature: Radial 104.6 cm and axial 886.7 cm.
- Xenon concentration: Radial 104.6 cm and axial 886.7 cm.

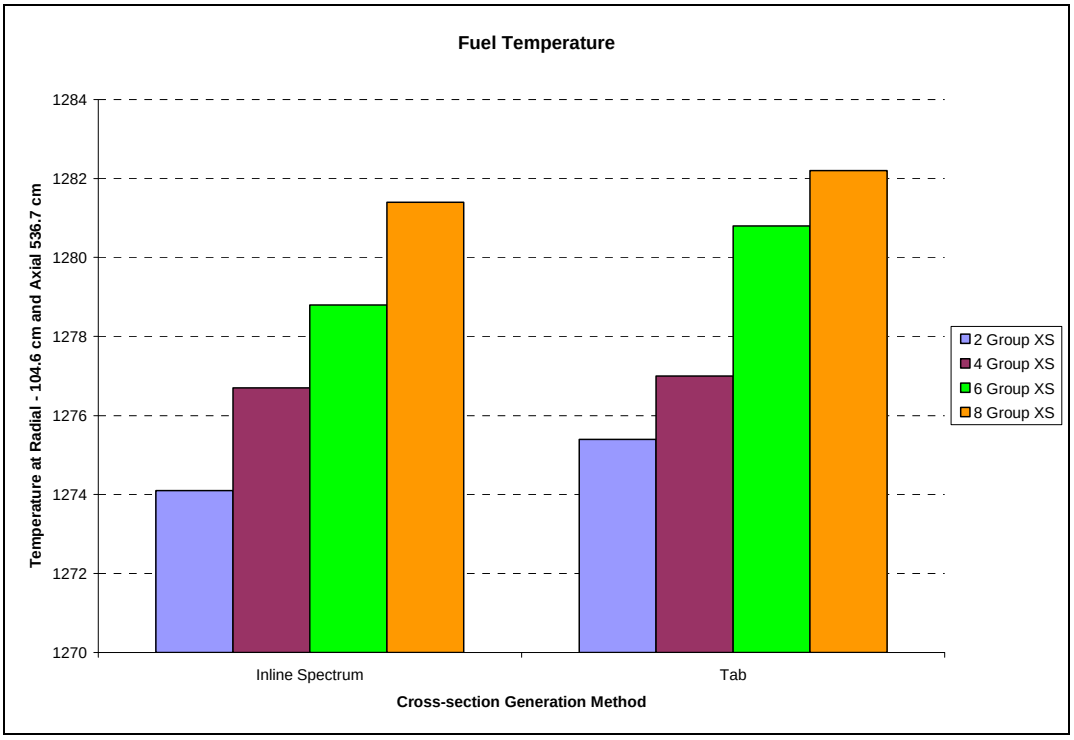

Figure 4-7: Steady state fuel temperature group structure comparison with cross-section generation methods

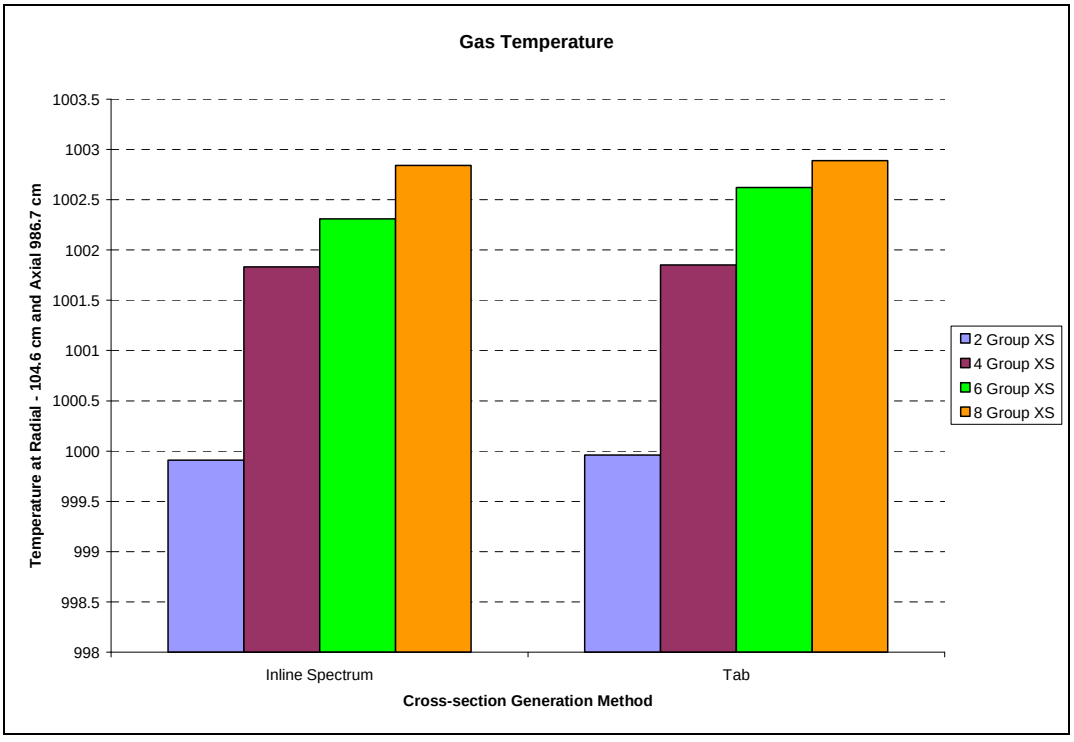

Figure 4-8: Steady state gas temperature group structure comparison with cross-section generation methods

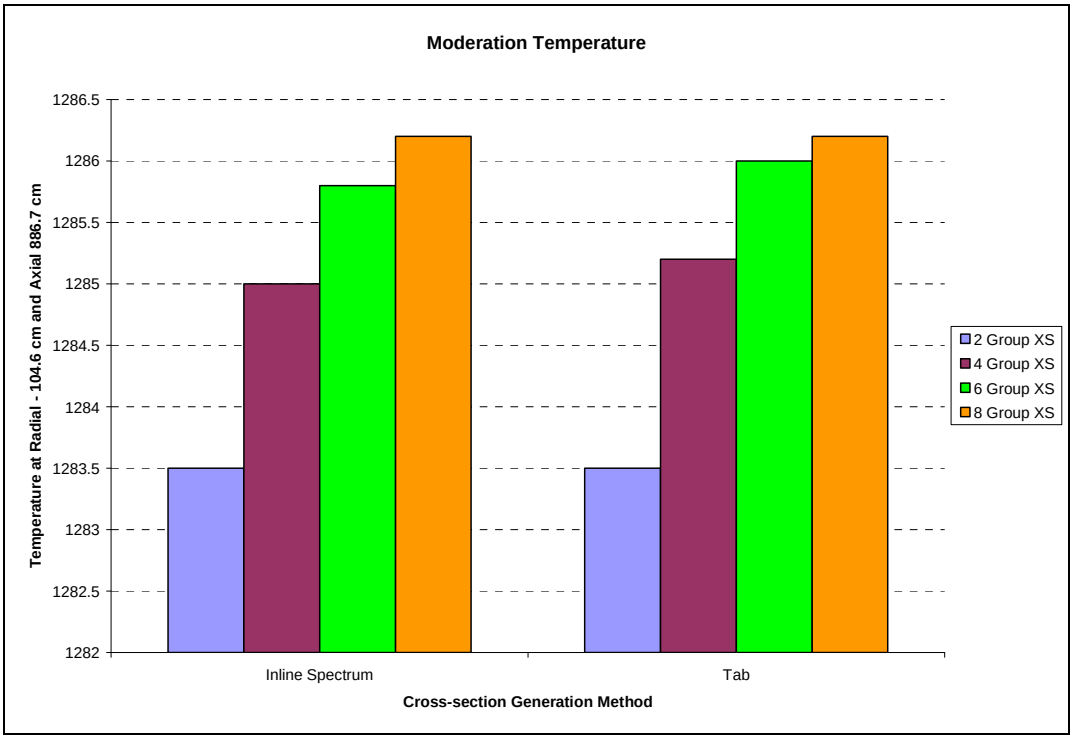

Figure 4-9: Steady state moderation temperature group structure comparison with cross-section generation methods

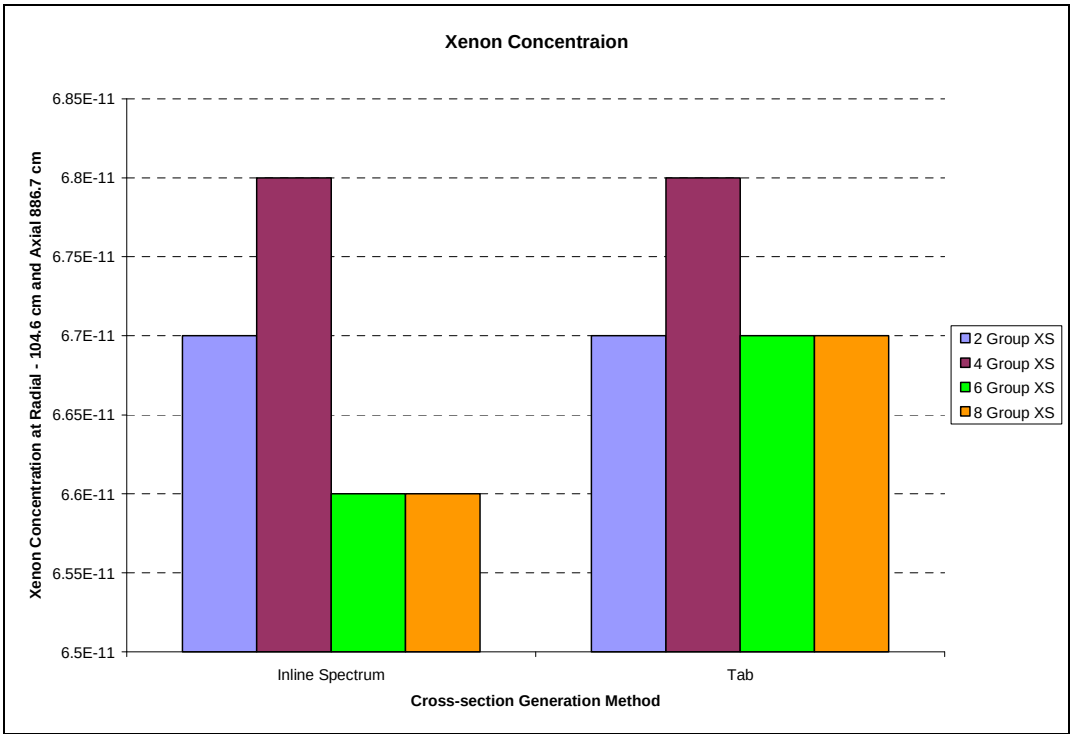

Figure 4-10: Steady state xenon concentration group structure comparison with cross-section generation methods

4.3 Conclusion

The fraction of delayed neutrons for Uranium-235 can change for low-enriched fuel from 0.007 to 0.0056 [2]. Therefore K-eff differences > 0.007 (700pcm) is highly significant for the safety of the reactor design.

As can be seen in Table 4-2, a significant error of 981 pcm for the 2-group Internal Spectrum can be seen if the 8-group Internal Spectrum calculation is taken as the Calculational reference.

The K-eff rapidly decreases to the insignificant level of -273 pcm and -121 pcm for the 4- and 6-group Internal Spectrum calculation respectively. Figure 1-2 shows the Internal Spectrum code calculations' CPU time have a small increase in CPU time from 2- to 4-groups, more to 6-groups and sinificantly to 8-groups.

Therefore a larger part of the available increase in accuracy can already be obtained with 4-groups, at the cost of only a small increase in CPU time. This balance between the accuracy and the calculation effort can be met. In other words the influence of group structure (changing the group structure from 2 to 8 groups) is greater than that of the cross-section generation methods applied, namely internal spectrum, table interpolation and the OECD cross-section. This can also be seen in Figure 4-7 to Figure 4-10.

5. CHAPTER FIVE: TRANSIENT INVESTIGATIONS

You may need some type of a roadblock to be placed in front of your progress so that you can become properly balance for the road you're to travel.
John Maxwell

5.1 Introduction

A discussion of the transient case can be recalled in 2.4.2. In the transient investigations, the cross-section generation methods and the energy group structures are the same as in the Steady state case which can be seen in 4.1 (steady state). Characteristics that will be compared include the following: reactor power, maximum fuel and moderation temperatures.

Fuel temperature is one of the most important safety parameters, since some radio-active fission products might leak through the coated particle at a temperature higher than 1600℃. Therefore the maximum fuel temperatur e will be the leading indicator in the results. In this specific transient of Control Rod Extraction or Reactivity Excursion the total maximum power is also important.

When using the table representation method and the changes in temperatures etc. are large, an interpolation error can be introduced and not all effects (especially no combined effects) can be represented by the tables. Whereas the detail fine group spectrum calculation is however repeated for the in-line spectrum calculation so that any inter-dependencies of few-group cross-sections to the conditions, are also taken into account. The 8-group Internal Spectrum results were taken as the selected calculational reference for comparison.

5.2 Results

5.2.1 *Reactor Power*

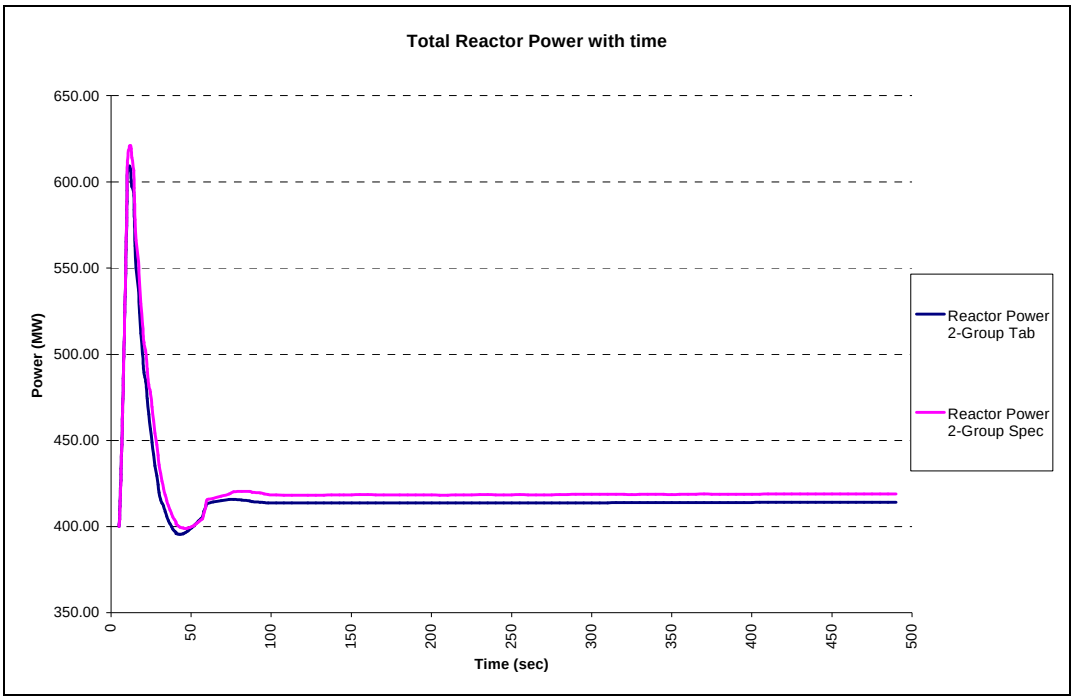

Figure 5-1: Reactor Power with time using 2-groups

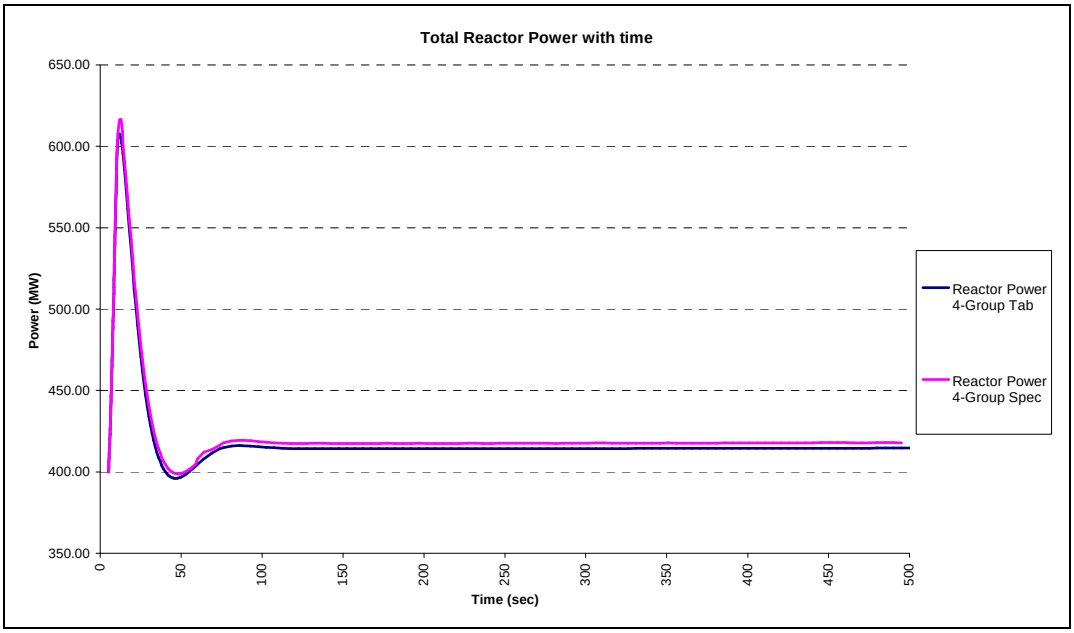

Figure 5-2: Reactor Power with time using 4-groups

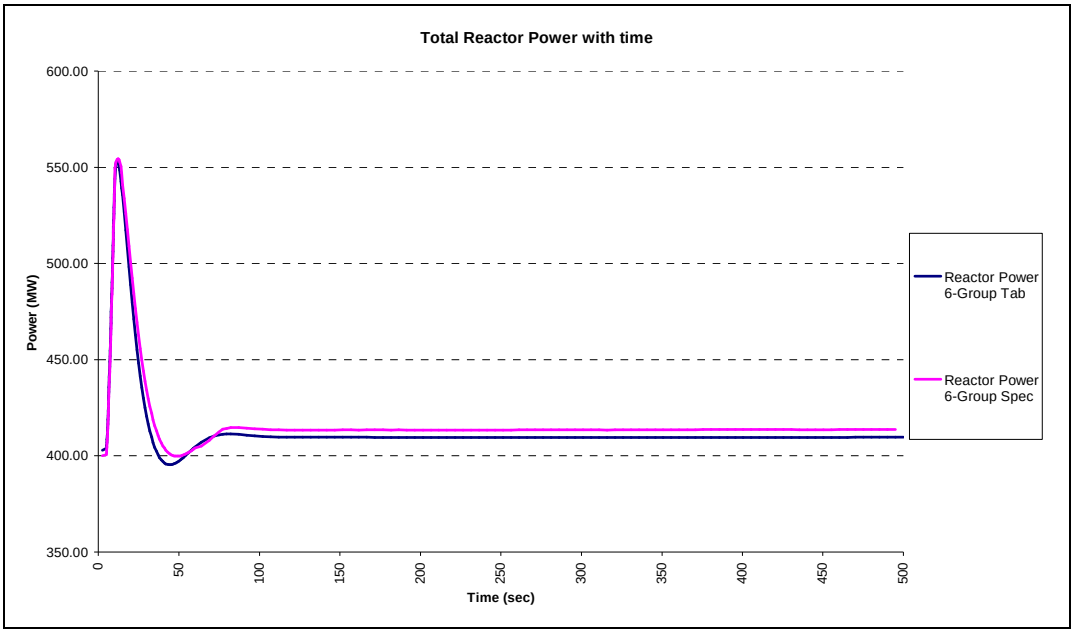

Figure 5-3: Reactor Power with time using 6-groups

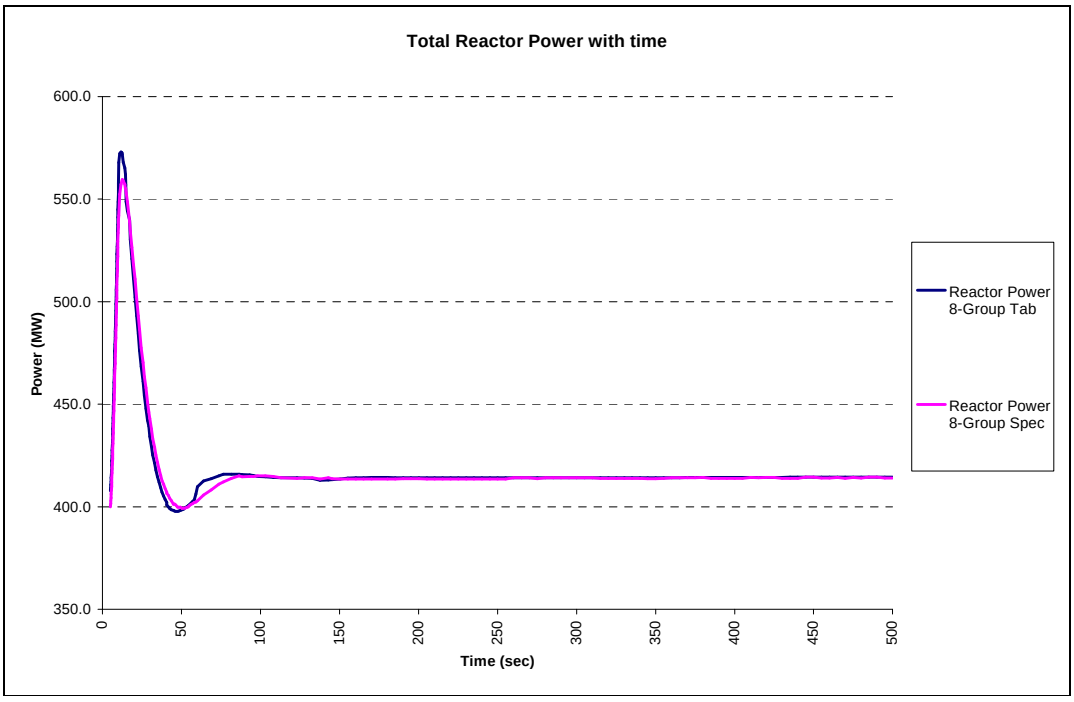

Figure 5-4: Reactor Power with time using 8-groups

Table 5-1: Reactor Power with 2, 4, 6 and 8 transient groups by using the internal spectrum and table interpolation cross-section generation methods

Case	Power	Difference in power in respect to 8-group Internal Spectrum (MW)
2-group Internal Spectrum	620.9	60.9
4-group Internal Spectrum	616.5	56.5
6-group Internal Spectrum	552.8	-7.2
8-group Internal Spectrum	560	
2-group Table Interpolation	606.5	46.5
4-group Table Interpolation	605.1	45.1
6-group Table Interpolation	552.5	-7.5
8-group Table Interpolation	571.8	46.5

5.2.2 *Maximum Fuel Temperature*

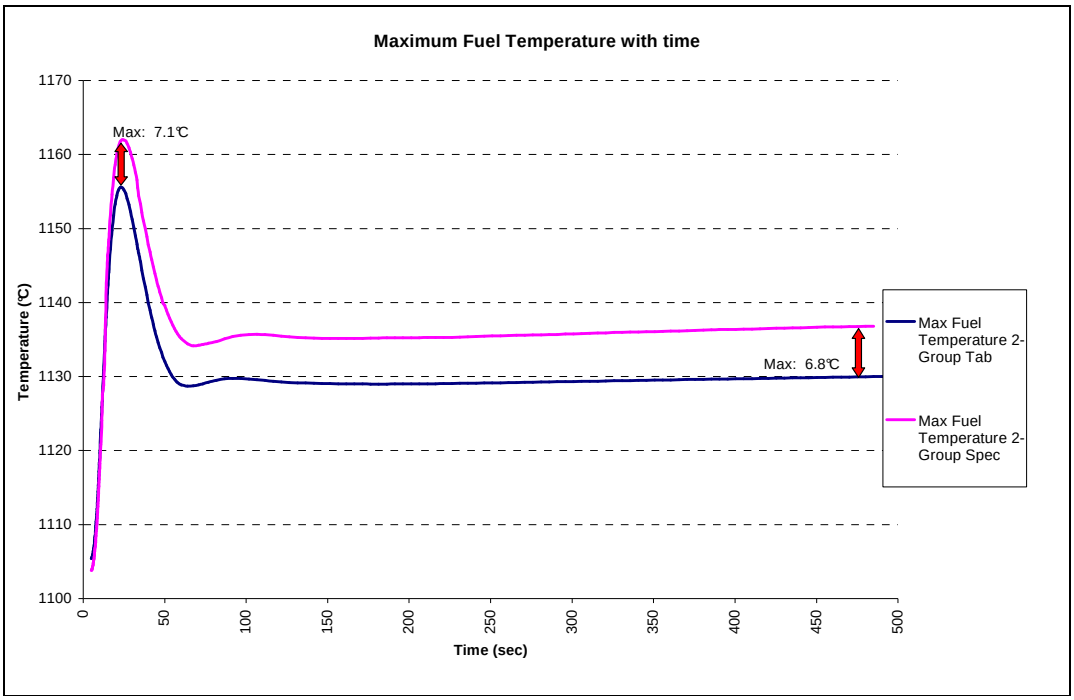

Figure 5-5: The difference in maximum fuel temperature with time using 2-groups.

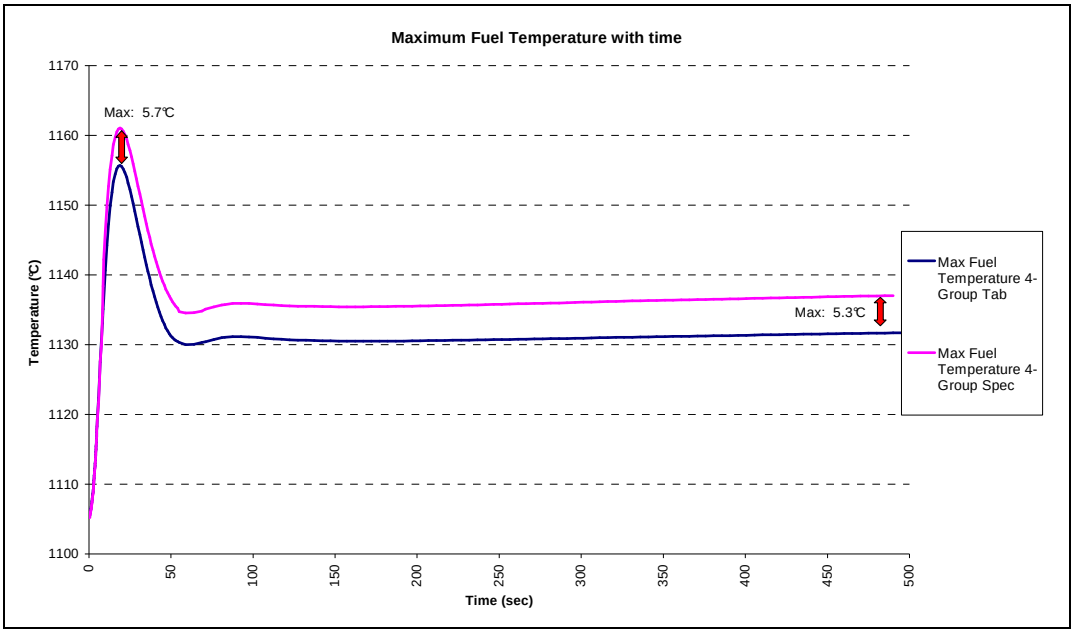

Figure 5-6: The difference in maximum fuel temperature with time using 4-groups.

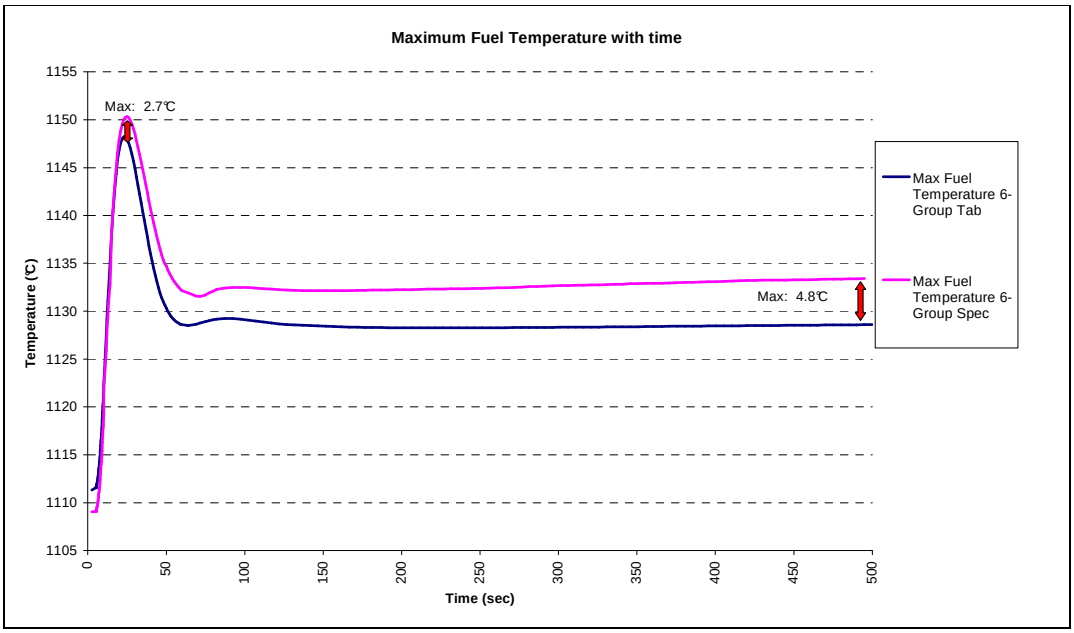

Figure 5-7: The difference in maximum fuel temperature with time using 6-groups.

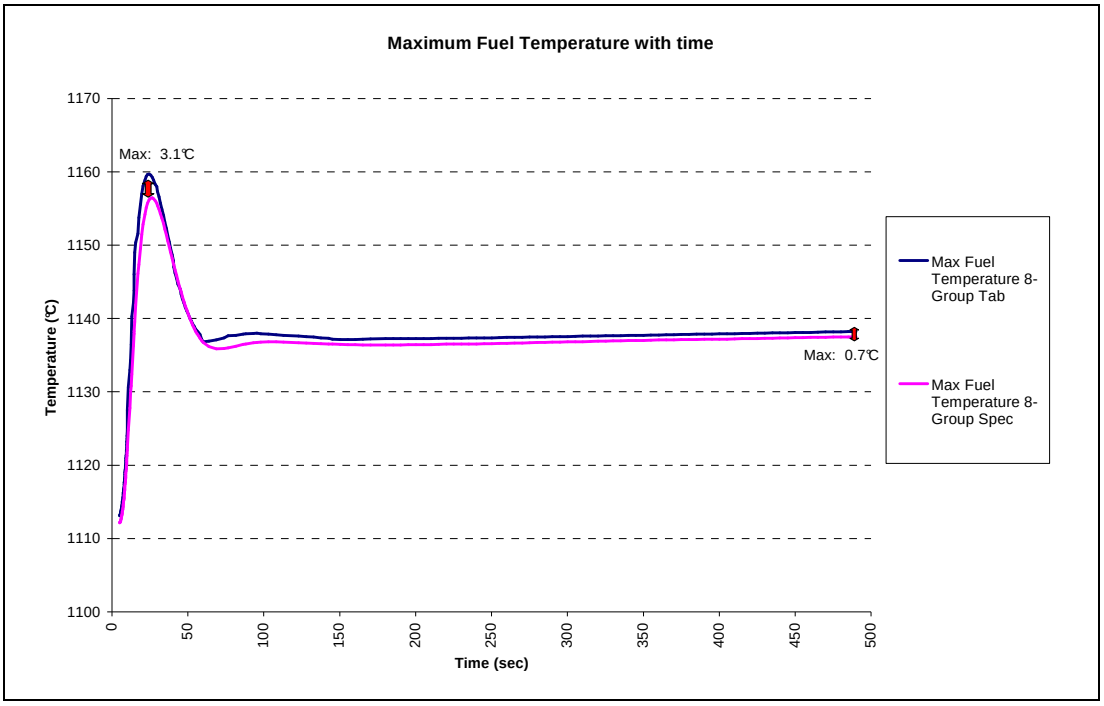

Figure 5-8: The difference in maximum fuel temperature with time using 8-groups.

Table 5-2: Maximum Fuel Temperature with 2, 4, 6 and 8 transient groups by using the internal spectrum and table interpolation cross-section generation methods

Case	Maximum Fuel Temperature	Difference in Maximum Fuel Temperature in respect to 8-group Internal Spectrum (℃)
2-group Internal Spectrum	1161.8	5.3
4-group Internal Spectrum	1160.9	4.4
6-group Internal Spectrum	1150	-6.5
8-group Internal Spectrum	1156.5	
2-group Table Interpolation	1154.7	-1.8
4-group Table Interpolation	1155.2	-1.3
6-group Table Interpolation	1147.3	-9.2
8-group Table Interpolation	1159.7	3.2

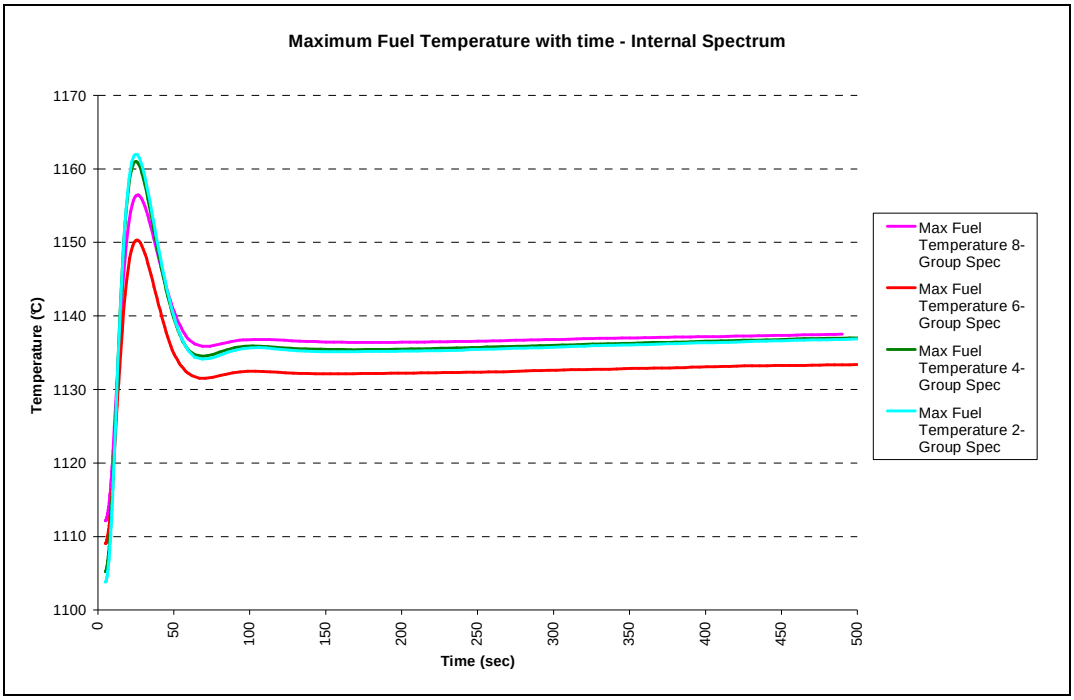

Figure 5-9: The maximum fuel temperature with time using different group-structures – Internal Spectrum Calculations

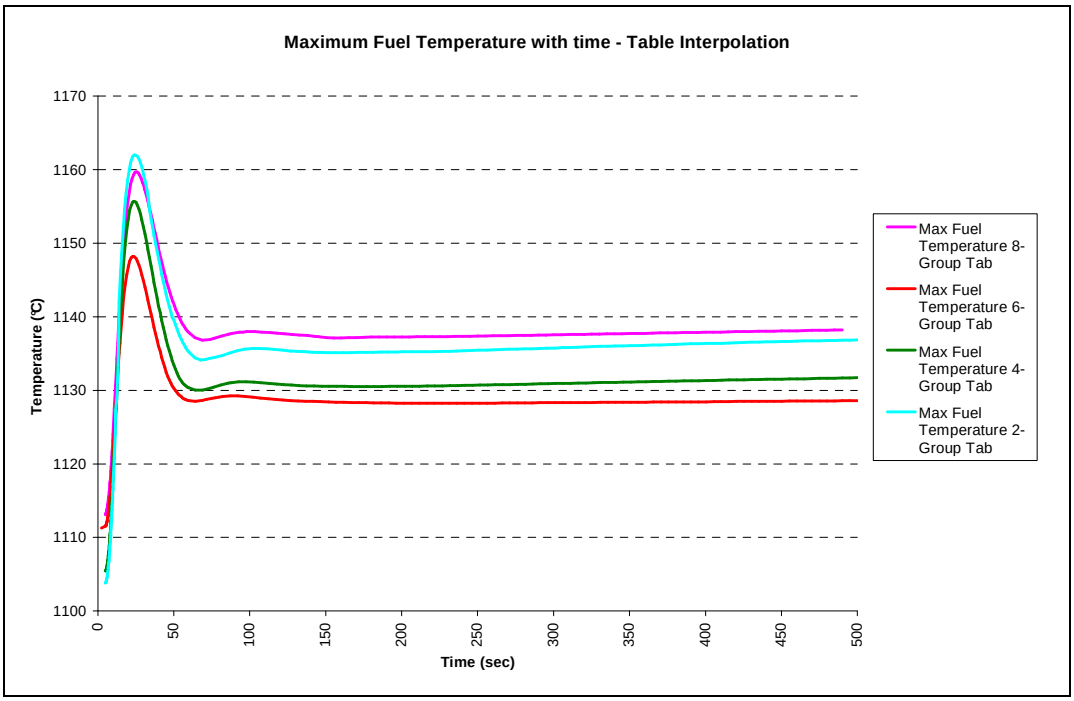

Figure 5-10: The maximum fuel temperature with time using different group-structures – Table Interpolation Calculations

5.2.3 *Moderator Temperature*

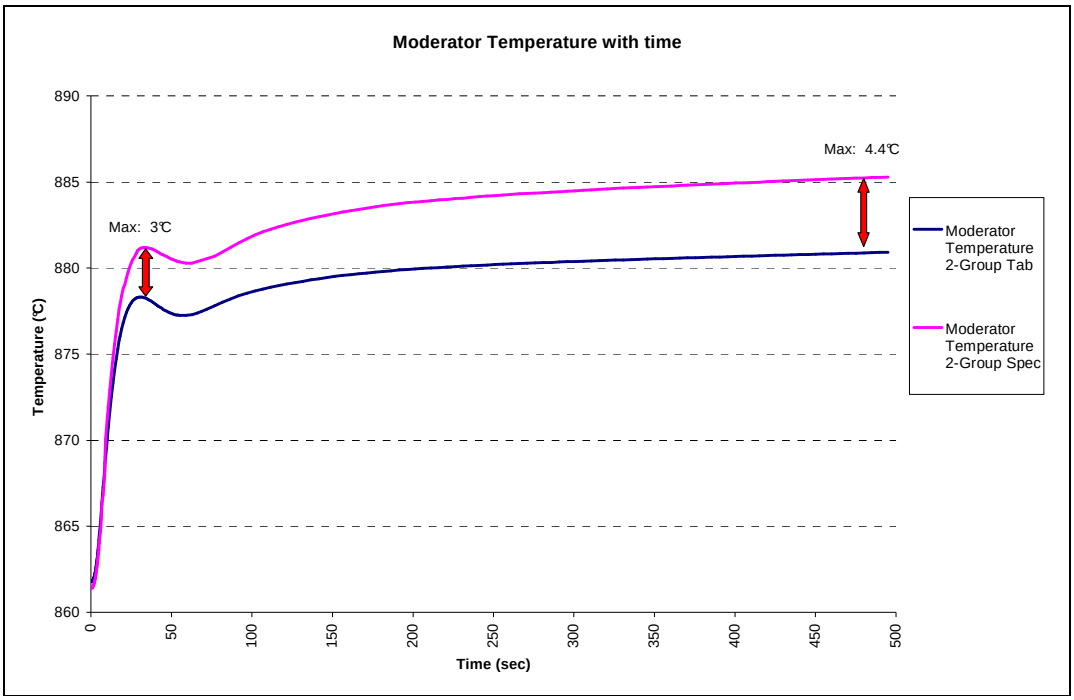

Figure 5-11: The difference in moderator temperature with time using 2-groups.

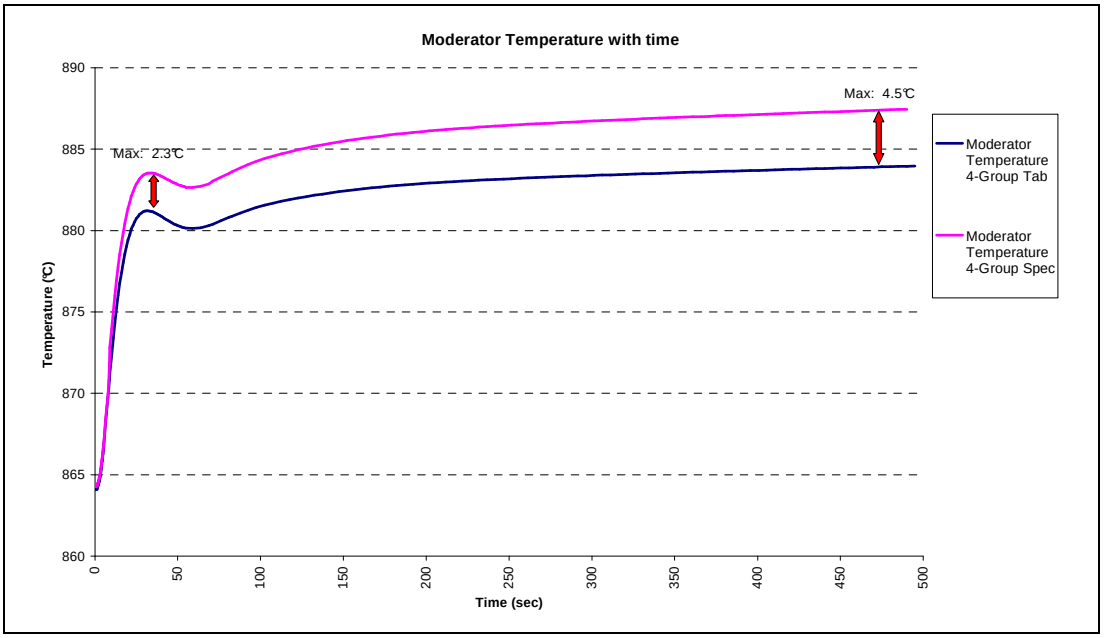

Figure 5-12: The difference in moderator temperature with time using 4-groups.

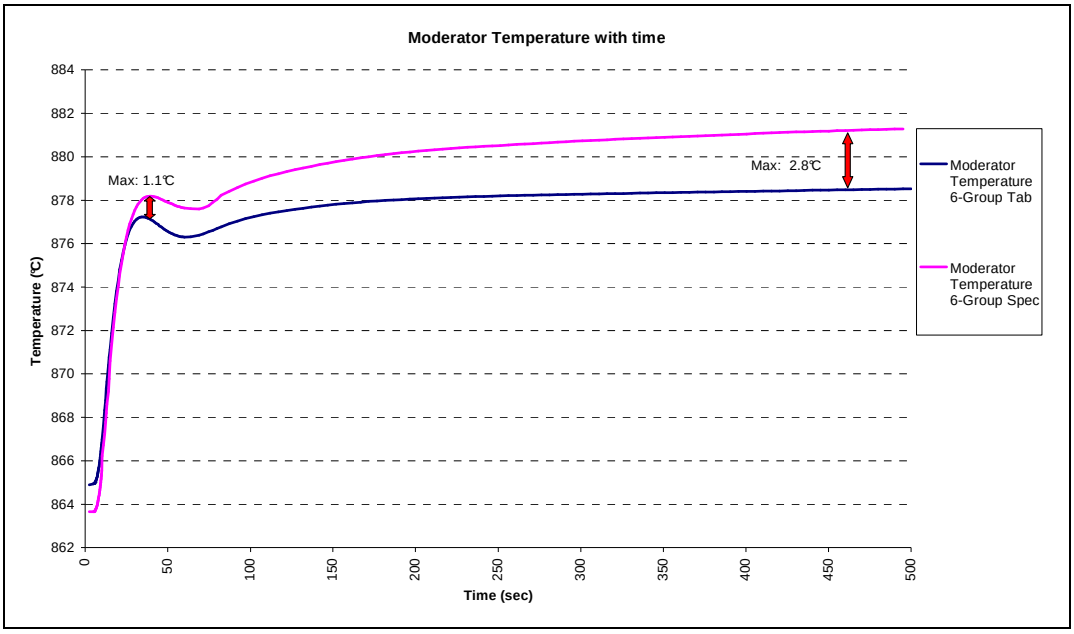

Figure 5-13: The difference in moderator temperature with time using 6-groups.

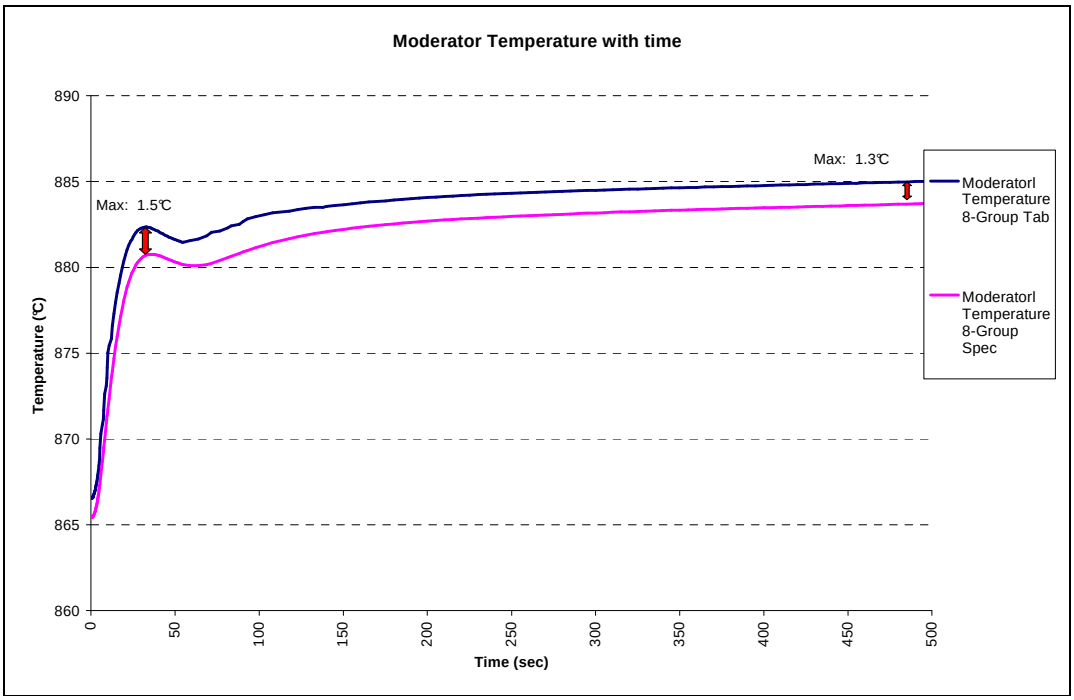

Figure 5-14: The difference in moderator temperature with time using 8-groups.

Table 5-3: Moderator Temperature with 2, 4, 6 and 8 transient groups by using the internal spectrum and table interpolation cross-section generation methods

Case	Moderator Temperature	Difference in Moderator Temperature in respect to 8-group Internal Spectrum (℃)
2-group Internal Spectrum	881.2	0.4
4-group Internal Spectrum	**883.5**	2.7
6-group Internal Spectrum	878.2	-2.6
8-group Internal Spectrum	**880.8**	
2-group Table Interpolation	878.2	-2.6
4-group Table Interpolation	**881.2**	0.4
6-group Table Interpolation	877.1	-3.7
8-group Table Interpolation	882.3	1.5

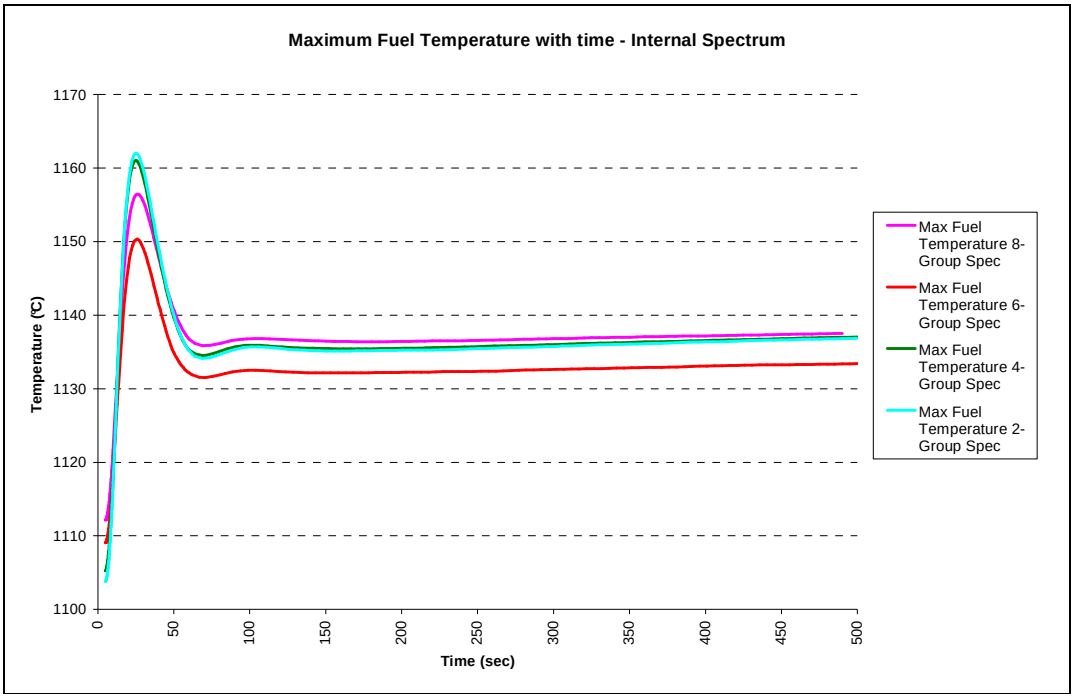

Figure 5-15: The maximum fuel temperature with time using different group-structures – Internal Spectrum Calculations

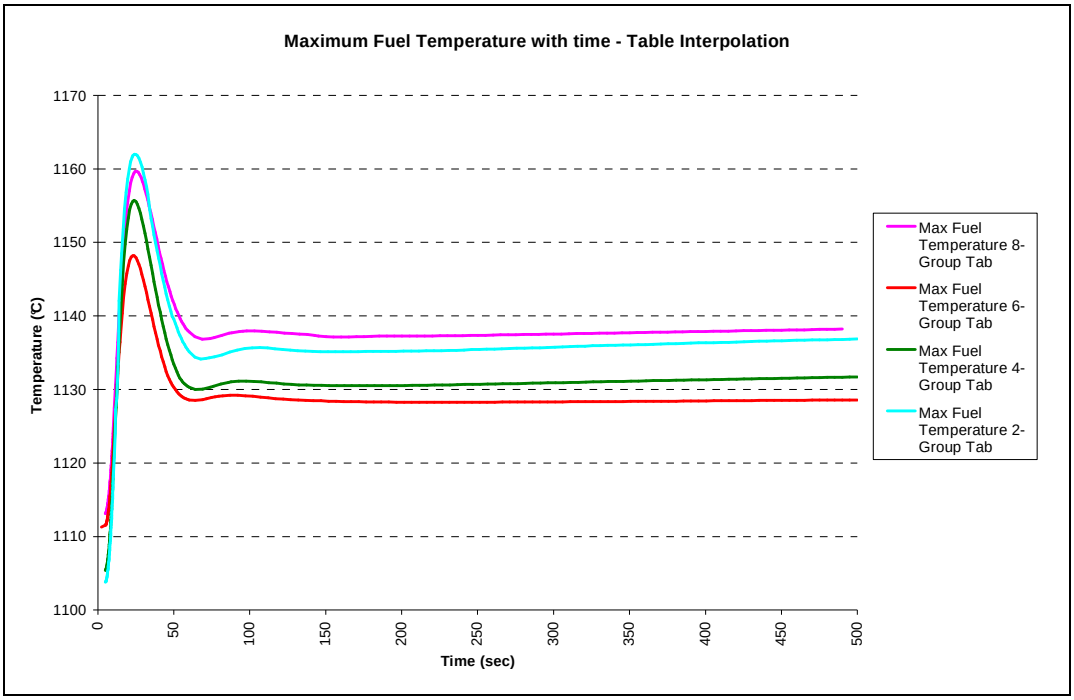

Figure 5-16: The maximum fuel temperature with time using different group-structures – Table Interpolation Calculations

5.3 Conclusion

In Figure 5-1 to Figure 5-4, when the 8-group Internal Spectrum results were taken as the selected calculational reference, increase in accuracy can be obtained with 6 groups, at the cost of a smaller increase in CPU time (refer to Figure 1-2), than with 8 groups. When calculating the reactor power, the influence of cross-section generation methods did not show such large sensitivity in the results. The number of energy groups had a big impact on the results from 2-groups to 8-groups.

The maximum fuel temperature comparison in Table 5-2, a large increase in accuracy can already be obtained with 4-groups, at the cost of only a small increase in CPU time (refer to Figure 1-2). It also shows that the cross-section generation methods influence the results more than the energy group division from 2- to 8-groups.

Table 5-3 shows a very small difference in results using 2- to 8-energy groups as well as the two different cross-section generation methods but the cross-section generation methods have an influence in the results than the energy groups division.

In Figure 5-1 to Figure 5-16 it can be seen that finer energy group structures give more accurate results when using the two different cross-section generation methods. In other words, the transient calculations show a larger sensitivity to the group structures than in the steady state results but have a similar effect on the cross-section generation method.

It can also be seen that the inline spectrum calculations tend to be higher than the function approximation by table interpolations. This is due to excess reactivity in the system (Clifford, 2007:27).

6. CHAPTER SIX: CONCLUSION AND RECOMMENDATION FOR FURTHER WORK

Sometimes prospects may seem dimmest just when they're on the turn. A little more persistence, a little more effort, and a hopeless failure may turn into a glorious success.
John Maxwell

6.1 Introduction

This chapter summarizes and presents the conclusions that emerged from this study. Recommendations for further work will also be made.

6.2 Conclusion

The objectives of this study were:

- To do a literature survey to help define the terms "one-group", "two-groups" and "multi-groups".
- To identify previous work done and current nuclear reactors' energy group structures.
- To do a comparative study between two-group TINTE and the equivalent two energy groups in MGT
- To do a comparative study with the under-mentioned two cross-section generation methods in conjunction with the group structures changing from 2, 4, 6 and 8 groups:
  - Internal spectrum code calculation.
  - Function approximation by table interpolations.
- To do an evaluation of the compared results and make the appropriate conclusion, whether the use of a multi-group energy structure is more accurate than a two-group structure and the influence of the:
  - energy group structures; and
  - cross-section generation methods.

These objectives have been successfully achieved and implemented. In this investigation several comparisons were made and the following conclusions were drawn.

6.2.1 *Steady state Calculations*

When steady state calculations are done with the multi-group dynamic energy code, MGT, special attention must be given to the group structure changes, in this case, 2 to 8 groups division. This study revealed that a balance between the accuracy and the calculation effort can be met with a 4-group energy division. In other words the influence of group structure (changing the group structure from 2 to 8 groups) is greater than that of the cross-section generation methods applied, namely internal spectrum, table interpolation and the OECD cross-section.

6.2.2 *Transient Calculations*

In the case of a transient calculation in MGT, cross-section generation methods are not to be neglected. The transient results show a larger sensitivity to the cross-section generation method than in the steady state case and has a similar effect as the number of energy groups. A balance between accuracy and calculation effort can be met with a 4- to 6-group internal spectrum cross-section generation methods.

6.2.3 *Final Conclusion*

When the energy group divisions changes from 2- to 4 groups, the thermal group (0.25E-0.2 eV - 0.03059 E+01 eV) was unchanged and the fast group (0.03059 E+01 eV – 0.1 E+08 eV) was divided into three smaller groups. The large improvement in accuracy from 2- to 4-groups implicates that the inaccuracy of the 2-group model lies primarily in the epithermal resonances. Therefore the most efficient way to improve the accuracy will be by neglecting the thermal region and focusing on the finer subdivision of the fast group region, with this in mind, please see recommendation for further work.

A balance between accuracy and calculation effort can be met by using a 4-group energy group structure in a steady state and transient calculation. A larger part of the available increase in accuracy can be obtained with 4-groups, at the cost of only a small increase in CPU time.

The influence of group structure plays a vital role at steady state calculation but in a transient calculation, cross-section generation methods as well as the number of energy groups are very important.

6.3 Recommendations for further work

A study where the thermal group (0.25E-0.2 eV - 0.03059 E+01 eV) is left unchanged, and higher energy group (0.03059 E+01 eV – 0.1 E+08 eV) can be divided into finer groups in the 6-, 8- and even 10-group cases.

Cross-section generation methods should be analyzed in a newer version of Multi-Group TINTE with the inclusion of the polynomial fit function cross-section generation method and other methods if available.

In the material zones of the specified model, five different cross-sectional-set types can be used (where a choice can be made for each material zone individually). The cross-section types that can be used are as follows (Gerwin *& Lauer*, 2007:2):

1. Input sets for internal Tispec spectrum calculations.
2. Tabulated data sets for linear cross-sections interpolation.
3. Coefficient sets for polynomial expansions of X-S themselves.
4. Similar for the expansion, not of the X-S themselves, but for the square roots of the X-S (in order to avoid negative fit values).
5. The logarithms of the X-S.

In combination of the above-mentioned five types of cross-section sets, each material zone can have an alternative cross-section set, to determine the impact of the different types of sets.

Variations in the materials' properties, such as thermal conductivity, effective thermal conductivity, heat capacity, etc., can be performed to determine the impact of the separate effects.

This study was performed with a group structure change from 2 to 8 energy groups. The influence of more than 10 energy groups should also be investigated.

7. CHAPTER SEVEN: REFERENCES

BERNARD, J. 2006. Course 22.05 Neutron Science and Reactor Physics: part twenty-three. *Neutron Science and Reactor Physics Lecture Notes*, MIT. Fall.

CLIFFORD, I. 2007. Calculation report, MGT preliminary testing results report, PBMR Internal Report, T000910, Rev B. July.

CLIFFORD, I. 2008. OECD PBMR 400MW transient benchmark cross-section representation option report, PBMR Internal Report, T01110, Rev A. February.

GARLAND, W.J. 2005. Nuclear Reactor Process Systems, Thermal-hydraulic Design, lectures: Design Requirements and Engineering Considerations, Reactor physics: multi-group diffusion. Department of Engineering Physics, McMaster University. Canada: Hamilton, Ontario. p. 4-6.

GERWIN, H. SCHERER, W. & TEUCHERT, E. 1989. The TINTE modular code system for computational simulation of transient processes in the primary circuit of a pebble-bed high temperature gas-cooled reactor. *Nuclear science and engineering,* 103:302-312.

GERWIN, H. & SCHERER, W. 2004 . TINTE users and programmers manual: TINTE version 204D. Centurion 140 p. (PP350-021998-3714).

GERWIN, H. & LAUER, A. 2007. Short Introduction to using the MGT Code. April.

GOUGAR, H.D., OUGOUAG, A.M. AND TERRY W.K. 2004. Advanced core design and fuel management for pebble bed reactors. Idaho National Engineering and Environmental Laboratory. Report Nr INEEL/EXT-04-02245). October.

GOUGAR, H.D. 2006. The application of the PEBBED code suite to the PBMR-400 coupled code benchmark. FY 2006 Annual Report. September.

JOHNSON, J.O. 1992. A users manual for Mash 1.0, a Monte Carlo adjoint shielding code system (contains the documentation for DORT). Oak Ridge National Laboratory Report ORNL/TM-11778.

KRIANGCHAIPORN, N. 2006. Transport model based on 3-D cross-section generation for TRIGA core analysis. Doctorial dissertation, The Pennsylvania State University.

LAUER, A. 2007. Meeting Presentation (FZJ/ISR): Multi-group energy models in HTR Computations with MGT: integral results and accuracy comparison. June 19.

NAKAGAWA, M. & MORI, T. 1992. Whole core calculations of power reactors by use of Monte Carlo method. Atomic Energy Research Institute, Japan. December. p. 84

NUCLEAR PHYSICS AND REACTOR THEORY Volume 1 of 2, Page 34, DOE-HDBK-1019/1-93

OECD/NEA/NSC PBMR COUPLED NEUTRONICS/THERMAL HYDRAULICS TRANSIENT BENCHMARK - THE PBMR-400 CORE DESIGN. 2007. Third workshop, NEA/NSC/DOC (2007)11, November.

REITSMA, F., IVANOV, K., DOWNAR, T., DE HAAS, H., SEN, S., STRYDOM, G., MPHAHLELE, R., TYOBEKA, B., SEKER, V., GOUGAR, H.D. & LEE, H.C. 2007. PBMR coupled neutronics/thermal hydraulics transient benchmark: the PBMR-400 core design, benchmark definition. Draft V07, to be published by OECD. NEA-1746/04, June.

ROUBEN, B. 2008. Nuclear reactor analysis. McMaster University, Canada: Hamilton, Ontario. Lecturers notes, EP 4D03/6D03, September – December. p. 3.

STOKER, C.C., REITSMA, F. & KARRIEM, Z. 2002. Creation of the equilibrium core PBMR ORIGEN-S cross-section library, Proceedings of HTR2002, Petten, The Netherlands, April.

TAKEDA, T. & IKEDA, H. 1991. 3-D neutron transport benchmarks. Department of Nuclear Engineering, Osaka University. March.

TYOBEKA, B., IVANOV, K. & PAUTZ, A. 2007. Utilization of two-dimensional deterministic transport methods for analysis of pebble-bed reactors, *Annals of nuclear energy* 34(2007):396–405, 27 March.

VARIN, E. & MARLEAU, G. 2006. CANDU reactor core simulations using fully coupled DRAGON and DONJON calculations. *Annals of nuclear energy* 33(2006):682–691, March.

TSUCHIHASHI, K. et al. 1986. Revised SRAC code system, JAERI-1302.

XINGGUAN, Z., JIANPING, C. & CHOW H.C. 1999. Physics codes and methods for CANDU reactor. China Journal of Nuclear Power Engineering 20(6).

Internet sources

[1] http://www.theengineer.co.uk/in-depth/classic-archive/october-1956-calder-hall-nuclear-station/294378.article

[2] http://www.pbmr.co.za/

[3] http://www.tpub.com/content/doe/h1019v2/index.htm